

ARCHIMEDES SCREW TURBINE MODEL
SIMULATION ON THE EFFECT OF
EXTERNAL AND INTERNAL DESIGN
PARAMETERS IN POWER GENERATION



NURUL SURAYA BINTI AZAHARI

UMP

اونيور سيني مابسيا قهغ
MASTER OF SCIENCE

UNIVERSITI MALAYSIA PAHANG
UNIVERSITI MALAYSIA PAHANG

UNIVERSITI MALAYSIA PAHANG

DECLARATION OF THESIS AND COPYRIGHT

Author's Full Name : NURUL SURAYA BINTI AZAHARI
Date of Birth : 04th NOVEMBER 1990
Title : ARCHIMEDES SCREW TURBINE MODEL
SIMULATION ON THE EFFECT OF EXTERNAL AND
INTERNAL DESIGN PARAMETERS IN POWER
GENERATION
Academic Session : SEMESTER 1 2021/2022

I declare that this thesis is classified as:


- CONFIDENTIAL (Contains confidential information under the Official Secret Act 1997)*
 RESTRICTED (Contains restricted information as specified by the organization where research was done)*
 OPEN ACCESS I agree that my thesis to be published as online open access (Full Text)

I acknowledge that Universiti Malaysia Pahang reserves the following rights:

1. The Thesis is the Property of Universiti Malaysia Pahang
2. The Library of Universiti Malaysia Pahang has the right to make copies of the thesis for the purpose of research only.
3. The Library has the right to make copies of the thesis for academic exchange.

Certified by:


(Student's Signature)


(Supervisor's Signature)

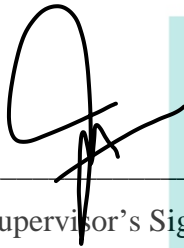
901104-06-5182
Date: 27 May 2022

TS. DR. UMMU KULTHUM
BINTI JAMALUDIN
Date: 27 May 2022

NOTE: * If the thesis is CONFIDENTIAL or RESTRICTED, please attach a thesis declaration letter.

SUPERVISOR'S DECLARATION

We hereby declare that we have checked this thesis and, in our opinion, this thesis is adequate in terms of scope and quality for the award of the degree of Master of Science.

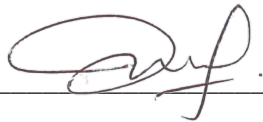


(Supervisor's Signature)

Full Name : TS. DR. UMMU KULTHUM BINTI JAMALUDIN

Position : SENIOR LECTURER

Date : 27 May 2022



(Co-supervisor's Signature)

Full Name : DR. NASRUL HADI BIN JOHARI

Position : SENIOR LECTURER

Date : 27 May 2022

اونیورسیتی ملیسیا قهق
UNIVERSITI MALAYSIA PAHANG

STUDENT'S DECLARATION

I hereby declare that the work in this thesis is based on my original work except for quotations and citations which have been duly acknowledged. I also declare that it has not been previously or concurrently submitted for any other degree at Universiti Malaysia Pahang or any other institutions.



(Student's Signature)

Full Name : NURUL SURAYA BINTI AZAHARI

ID Number : MMM 14023

Date : 27 May 2022

UMP

اونيورسيتي ملايسيا قهغ

UNIVERSITI MALAYSIA PAHANG

ARCHIMEDES SCREW TURBINE MODEL SIMULATION
ON THE EFFECT OF EXTERNAL AND INTERNAL
DESIGN PARAMETERS IN POWER GENERATION



Thesis submitted in fulfillment of the requirements
for the award of the degree of
Master of Science

اونيورسيتي مليسيا قهغ

UNIVERSITI MALAYSIA PAHANG

Faculty of Mechanical and Automotive Engineering Technology

UNIVERSITI MALAYSIA PAHANG

MAY 2022

ACKNOWLEDGEMENTS

After a long journey of my Master's studies, today is the day; I am writing this acknowledgement to thank all the people that have contributed and supported me throughout this journey.

First and foremost, I would like to thank my main supervisor and co-supervisor, Dr. Ummu Kulthum binti Jamaluddin and Dr. Nasrul Hadi bin Johari, respectively, for their guidance and encouragement. Both supported me a lot in the aspects of morality, cooperation, ideas, and financing. Besides, a big thank you to my ex-co-supervisor, Mr. Muhammad Ammar bin Nik Mu'tasim, for the valuable ideas, time, and support while supervising me before furthering his studies. I am so grateful to have them as my main and ex-co-supervisors.

I would like to express my sincere gratitude to my lovely parents for their love, dreams, support, and sacrifice throughout my life. I just cannot find the appropriate words to describe their kindness and amazing support. Family support is the best catalyst in the world.

Besides, I would like to thank Dr. Ahmed Nurye Oumer for sharing his knowledge and time. My sincere thanks also go to all my group mates and members of the staff of the Faculty of Mechanical and Automotive Engineering Technology, Universiti Malaysia Pahang, who helped me in many ways, such as installing the software that I needed on my laptop and making my work easier. Many special thanks go to the Energy Sustainable Focus Group (ESFG) members for their support, cooperation, and idea sharing during this study.

Finally, to my friends who have always supported me throughout my studies. You guys are so awesome.

اونيورسيتي ملايسيا قهغ

UNIVERSITI MALAYSIA PAHANG

ABSTRAK

Tahun demi tahun, permintaan elektrik meningkat disebabkan oleh pertumbuhan pesat dunia, yang menggunakan elektrik sebagai sumber tenaga utamanya. Untuk mengatasi cabaran menjana elektrik dari sumber tenaga konvensional yang menyumbang kepada kesan rumah hijau, tenaga boleh diperbaharui boleh digunakan. Salah satu alternatif untuk menjana elektrik dalam persekitaran yang bersih ialah turbin skru Archimedes (AST). Objektif kajian penyelidikan ini adalah untuk menyiasat sudut kecenderungan cerun AST, nisbah diameter, dan bilangan skru bilah berdasarkan konsep reka bentuk sebelumnya untuk penjaan kuasa dan menentukan penjaan kuasa dan kecekapan tertinggi berdasarkan parameter dalaman dan luaran. Penyelidikan ini bertujuan untuk mengkaji konsep reka bentuk AST untuk menjana elektrik. Konsep reka bentuk dianalisis berdasarkan parameter geometri, yang kemudiannya disahkan antara simulasi dan data sebenar. Tiga parameter yang dipertimbangkan dalam penyelidikan ini adalah sudut kecenderungan cerun, nisbah diameter, dan bilangan skru bilah. Setiap parameter mempengaruhi penjaan kuasa AST dengan ketara. Simulasi konsep reka bentuk AST telah dijalankan menggunakan ANSYS CFX. Simulasi ini dibahagikan kepada beberapa langkah, seperti pengesahan antara simulasi dan data eksperimen, dan simulasi AST menggunakan tiga parameter yang berbeza pada kadar aliran malar dan kelajuan putaran. Sebanyak 36 simulasi dijalankan berdasarkan kadar aliran malar dengan beberapa skru bilah 1, 2 dan 3, dengan nisbah diameter 0.25, 0.5 dan 0.6 digabungkan dengan sudut kecenderungan cerun 20° , 25° , 35° dan 40° . Daripada simulasi, kuasa tertinggi 2.3W dihasilkan pada 1 skru bilah, $0.5D_r$ dan 40° , manakala kecekapan tertinggi (79.42%) berlaku pada 3 skru bilah, 20° dan $0.25D_r$. Setiap reka bentuk kajian parameter memberi kesan kepada pengeluaran kuasa dan kecekapan AST.

اونيورسيتي مليسيا قهغ

UNIVERSITI MALAYSIA PAHANG

ABSTRACT

Year after year, electricity demand increases due to the world's rapid growth, which uses electricity as its main source of energy. In order to overcome the challenge of generating electricity from conventional energy resources that contribute to the greenhouse effect, renewable energy is in demand. One of the alternatives to generating electricity in a clean environment is the Archimedes screw turbine (AST). The objective of this research study is to investigate the AST slope inclination angle, diameter ratio, and number of bladed screws based on previous design concepts for power generation and determine the power output and highest efficiency based on the internal and external parameters. This research is aimed at studying the AST design concept for generating electricity. The design concept was analysed based on the geometric parameters, which were then validated between the simulation and actual data. Three parameters considered in this research were the slope inclination angle, α ratio of diameter, D_r and number of bladed screws, N . Each parameter affects the AST power generation significantly. The simulation of the AST design concept was carried out using ANSYS CFX. The simulation was divided into several steps, such as validation between the simulation and experimental data, and simulation of the AST using three different parameters at a constant flow rate and rotational speed. A total of 36 simulations were run based on constant flow rate with a number of bladed screws of 1, 2 and 3, with a diameter ratio of 0.25, 0.5 and 0.6 combined with a slope inclination angle of 20° , 25° , 35° and 40° . From the simulation, the highest power of 2.3W was produced at 1 bladed screw, 0.5 D_r and 40° , whereas the highest efficiency (79.42%) occurred at 3 bladed screws, 20° and 0.25 D_r . Each of the designs of the parameter studies impacted the power production and efficiency of AST.

UMP

اونيورسيتي ملايسيا قهغ

UNIVERSITI MALAYSIA PAHANG

TABLE OF CONTENT

DECLARATION

TITLE PAGE

ACKNOWLEDGEMENTS **ii**

ABSTRAK **iii**

ABSTRACT **iv**

TABLE OF CONTENT **v**

LIST OF TABLES **viii**

LIST OF FIGURES **ix**

LIST OF SYMBOLS **x**

LIST OF ABBREVIATIONS **xi**

CHAPTER 1 INTRODUCTION **1**

1.1 Introduction 1

1.2 Problem Statement 3

1.3 Objectives of the Study 4

1.4 Scopes of the Study 4

1.5 Summary 5

CHAPTER 2 LITERATURE REVIEW **7**

2.1 Introduction 7

2.2 Renewable Energy 7

2.3 Hydropower Plant 9

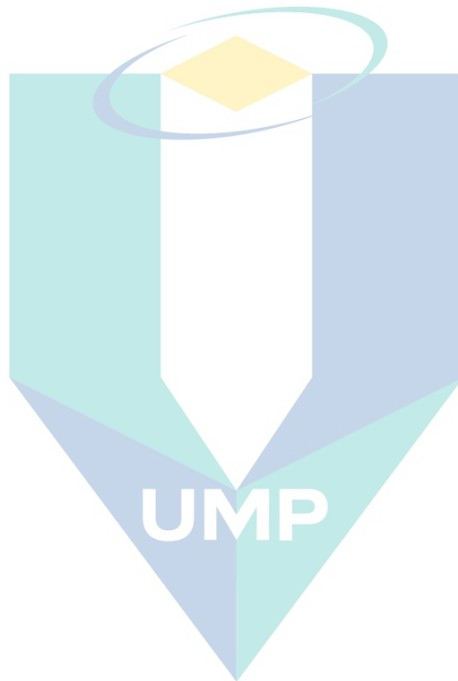
2.4 Archimedes Screw Runner Blade 10

2.4.1 History of the Archimedes Screw Runner Blade as a Pump and Turbine 10

2.4.2 Advantages of the Archimedes Screw Turbine 12

2.4.3	Concept of Archimedes Screw Turbine Application	13
2.5	Parameter Studied for AST	16
2.6	Computational Fluid Dynamics (CFD)	27
CHAPTER 3 METHODOLOGY		30
3.1	Introduction	30
3.2	Simulation of Parameter Selection	35
3.2.1	Independent Parameter	36
3.2.2	Internal Parameters	37
3.2.3	External Parameters	37
3.3	Dimensional Analysis	37
3.4	Computational Fluid Dynamics Simulation	38
3.4.1	Simulation Set Up	39
3.4.2	Meshing Sensitivity	47
3.4.3	Simulation Convergence Criteria	49
3.5	Calculation for Power Output and Efficiency of AST	50
CHAPTER 4 RESULTS AND DISCUSSIONS		52
4.1	Introduction	52
4.2	Model Validation	53
4.3	Results for N=1, 2 and 3	54
4.3.1	At N=1	54
4.3.2	At N=2	56
4.3.3	At N=3	58
4.4	Efficiency of the AST	59
4.5	Summary of the Findings	62

CHAPTER 5 CONCLUSION AND RECOMMENDATION	63
5.1 Conclusion	63
5.2 Recommendation	63
REFERENCES	65
APPENDICES	70

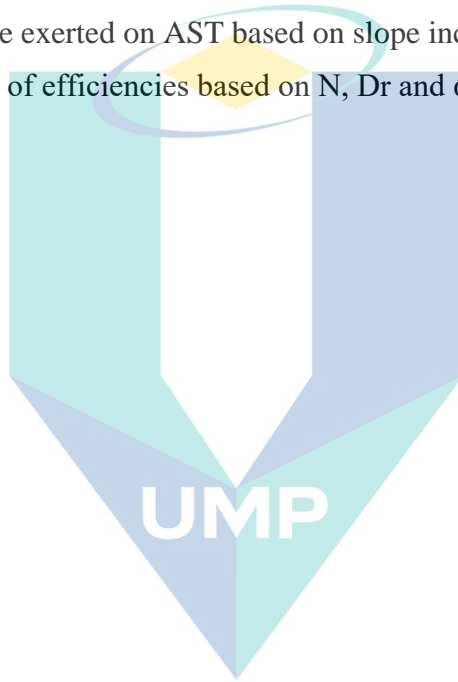


اونيورسيتي ملايسيا قهغ

UNIVERSITI MALAYSIA PAHANG

LIST OF TABLES

Table 2.1	Classification of hydropower plants	9
Table 2.2	Summary of parameters studied by previous researcher	19
Table 3.1	Dimensions of the AST model	36
Table 3.2	Geometric parameters for the simulation study	37
Table 3.3	Type of quality and the level of accuracy	45
Table 3.4	Torque generated from the simulation and corresponding percentage error	48
Table 4.1	Pressure exerted on AST based on slope inclination angle	54
Table 4.2	Results of efficiencies based on N , D_r and α	59



اونيورسيتي ملايسيا قهغ

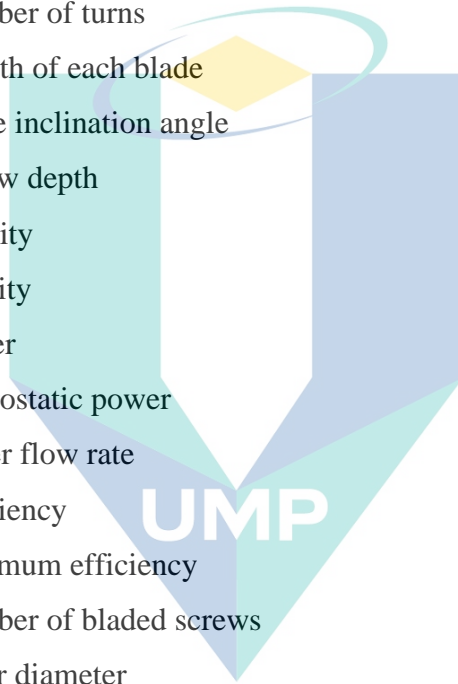
UNIVERSITI MALAYSIA PAHANG

LIST OF FIGURES

Figure 2.1	Malaysia's primary energy consumption in 2011	8
Figure 2.2	Schematic diagram of a micro hydroelectric power plant	10
Figure 2.3	A three-bladed Archimedes screw runner pump	11
Figure 2.4	Side view of the Archimedes screw turbine	12
Figure 2.5	Classification of head and water flow rates for different types of turbines	13
Figure 2.6	Energy conversion of Archimedes Screw Turbine (AST)	14
Figure 2.7	Side view of the AST diagram	14
Figure 3.1	Research flow chart	31
Figure 3.2	Geometrical parameters of the AST model	36
Figure 3.3	Schematic diagram of CFD elements	39
Figure 3.4	Details project schematic using ANSYS CFX	40
Figure 3.5	Cross section - stationary part of the flow	41
Figure 3.6	Cross section - rotating part of the blades	41
Figure 3.7	Boundary condition applied	42
Figure 3.8	Coarse, medium, and fine relevance center of meshing	43
Figure 3.9	Meshing of blade part	44
Figure 3.10	Close up of the meshing of blade part	44
Figure 3.11	RMS Residual curve	49
Figure 4.1	Comparison between simulation and experimental data using three different slope inclination angles	53
Figure 4.2	Power output of AST for different slope inclination angle and diameter ratio with constant $N=1$	55
Figure 4.3	Power output of AST for different slope inclination angle and diameter ratio with constant $N=2$	57
Figure 4.4	Power output of AST for different slope inclination angle and diameter ratio with constant $N=3$	58

LIST OF SYMBOLS

P_{blade}	Power of each blade
F_{hyd}	Hydrostatic force
v_1	Approach velocity
v_0	Inlet speed
Δd	Water depth
H	Head different
m	Number of turns
l	Length of each blade
α	Slope inclination angle
d_0	Inflow depth
ρ	Density
g	Gravity
P	Power
P_{hyd}	Hydrostatic power
Q	Water flow rate
η	Efficiency
η_{min}	Minimum efficiency
N	Number of bladed screws
D_o	Outer diameter
D_i	Inner diameter
P	Pitch diameter
s	Gap between blade and trough
D_r	Diameter ratio
T	Torque
ω	Rotational speed
L	Length of the screw



اونیورسیتی ملیسیا فہق

UNIVERSITI MALAYSIA PAHANG

LIST OF ABBREVIATIONS

AST	Archimedes Screw Turbine
BC	Before Christ
CAD	Computer-Aided Design
CFD	Computational Fluid Dynamics
CV	Control Volume
DNS	Direct Numerical Simulation
FVM	Finite Volume Method
K-S	Kolmogorov-Smirnov
LES	Large Eddy Simulation
MLR	Multi-Linear Regression
RANS	Reynolds-Averaged Navier-Stokes
RE	Renewable Energy
Re	Reynolds Number
VOF	Volume of Fraction
CO ₂	Carbon Dioxide



اونيورسيتي مليسيا قهق

UNIVERSITI MALAYSIA PAHANG

CHAPTER 1

INTRODUCTION

1.1 Introduction

Energy is important in daily life. Energy is the ability to do work, and energy cannot be created or destroyed but can be transferred from one form into another. The forms of energy can be classified into kinetic, potential, mechanical, nuclear, ionization, chemical, electromagnetic, sonic, and gravitational. Two types of useful energy are conventional and non-conventional energy. Conventional energy is the energy source that cannot be replaced after use. Non-conventional energy is renewable energy (RE). The use of RE has achieved a major breakthrough due to the growing fossil fuel demand, which is estimated to decline by 2020 (Mekhilef, 2010; Ong et al., 2011). Nowadays, RE sources commonly used to replace the use of conventional energy include solar, geothermal, biomass, biofuels, wind, hydro, and fuel cells (Bilotta et al., 2017; Keawsuntia, 2014; McNabola et al., 2014). All these energy sources will never diminish and have a high potential to produce a clean environment and reduce greenhouse gas emissions.

Renewable energy is particularly suitable for developing countries, especially in rural and remote areas where the distribution of energy from fossil fuels is expensive.

Therefore, the use of RE can be one of the alternative ways to overcome this problem. Five sectors of energy consumption in Malaysia are residential (12%), industrial (35%), commercial (19%), transportation (32%), and agriculture (2%). In the residential sector, people use energy in their daily lives for cooking equipment, refrigerators, air conditioners, washing machines, and others (C. Chong et al., 2015).

Generally, the Earth is covered by more than 70% of water; therefore, this energy source should be fully exploited. Hydro power is one of the useful energy sources generated from a water source. In general, hydropower plants can be classified into large,

medium, small, mini, micro, and pico hydropower plants, which can generate electricity up to more than 100 MW, 15–100 MW, 1–15 MW, 100 kW–1 MW, 5–100 kW, and 100 W–5 kW, respectively (Keawsuntia, 2014; Mohibullah, 2004; Raza & Mian, 2013). Most hydropower plants need dams and water reservoirs to generate electricity, except for micro and pico hydropower plants that are classified as run-of-river hydropower plants (Furukawa et al., 2010).

Hydropower energy is generated from the water source where the turbine is needed to transform the energy in flowing water into useful energy such as electricity. Generally, Malaysia should use the source of water by using this hydropower energy substantially as this country rarely experiences the phenomenon of drought. Hence, the water turbine is needed to generate electricity from the water source. There are several types of turbines, such as Turgo, Crossflow, Pelton, Francis, Kaplan, and Archimedes. Each of the turbines has a various head difference, where the Archimedes screw turbine (AST) has the lowest head (10m). In this study, the Archimedes Screw Turbine (AST) turbine was chosen due to its focus on rural and remote areas for power generation.

Commonly, an Archimedes screw turbine (AST) is one of the potential selections to produce a hydro turbine due to its low maintenance, environmentally friendly, and good efficiency for high flow rates and low heads (Bambang Yulistiyanto, Yul Hizhar, 2012; Elbatran et al., 2015; McNabola et al., 2014). Besides, this AST is also categorised as run-of-river, where the design does not require a large reservoir and the power is also free of carbon dioxide (CO₂) emission. The AST is categorised as a reaction turbine where the ratio of static pressure drops across the rotor and the static drops across the turbine state (Barelli et al., 2013). The primary feature of the AST is that the weight of water enclosed by the screw's blade makes the blade rotate due to kinetic energy. Meanwhile, the turbine turns the generator rotor to convert mechanical energy into electrical energy. Theoretically, the AST can obtain 100% efficiency by assuming no losses (Muller & Senior, 2009). However, it is impossible to obtain 100% efficiency by experiment or simulation method as there will be several factors that may impact the performance. Besides, there are several disadvantages to this AST. For example, it requires high flow and the oversized turbine can also lead to no electricity production.

Hence, it is important to ensure that the selection of the geometry is properly significant in power production.

There are a lot of factors that may affect the performance of the turbine, but in this study, the parameters of the AST design are of concern. The parameters of AST can be classified into internal and external. External parameters include the outer diameter of the blade and the slope inclination angle, whereas internal parameters consist of the inner diameter, number of turns, and pitch of the blade. Rorres (2000) and Shimomura & Takano (2013) concluded that flow geometry and turbine rotation have a substantial effect on torque. Muller & Senior (2009) investigated the effects of losses and blade geometry, and they observed increased efficiencies at a lower inclination angle with an increasing number of turns. The study on the slope inclination angle was performed by Bambang Yulistiyanto and Yul Hizhar (2012) experimentally, and they found the optimum slope inclination angle at an average angle of 35° at high water flow rates. There are some contradictory findings on the slope inclination angle between the two researchers (i.e., using theoretical and experimental methods). Therefore, in this study, three parameters were investigated and studied to identify whether these parameters have a significant impact on the power production of the AST.

1.2 Problem Statement

As the world advances, electric power consumption also increases, while conventional energy consumption decreases (i.e., fossil fuels). Hence, an approach to overcome these problems is to use free natural RE sources, such as hydro power, where water can generate electricity by using the AST. Micro hydropower is the source of energy that helps to minimise the reliance on fossil fuels while lowering greenhouse gas emissions significantly. Hence, to solve the problem of diminishing fossil fuels, the AST can be used to generate electricity in rural and remote areas. There are some factors that affect the power production from AST, and in this research study, the parameters of AST are concerned. Three parameters, such as slope inclination angle, the number of the bladed screws, and the diameter ratio, are studied.

Numerically (using Matlab software), Shahverdi et al., (2020) concluded that a single number of blades with a 20° inclination angle would produce the highest

efficiencies (90.83%). Other researchers found that four and five blades with an angle of 20° to 24° would generate the highest efficiencies, at 87%, using the CFD software OpenFOAM (Dellinger et al., 2019). Meanwhile, Siswantara et al., (2019) experimentally obtained contradicting results, where the inclination angle of the turbine does not significantly affect the performance of the AST, focusing more on the load exerted on the AST. Other than the slope inclination angle and number of blades, screw geometry is also vital to producing maximum efficiency theoretically (Muller & Senior, 2009).

Even though many numerical, experimental, and simulation studies have been conducted on the parameters, the comparison between these three parameters remains unsolved. The power output of the AST can be generated using the simulation method (ANSYS CFX). Meanwhile, the efficiency of the AST is determined by the ratio of power output versus power input derived from the flowrate of the water entering the AST. The purpose of this study is to identify the highest power output produced by AST and its efficiency based on the internal and external AST design parameters.

1.3 Objectives of the Study

The objectives of this study are:

- i. To investigate the AST slope inclination angle, diameter ratio, and number of bladed screws based on the previous design concept for power generation (two internals and one external geometric parameter).
- ii. To simulate the AST design concept using slope inclination angle, diameter ratio, and number of bladed screws based on constant flowrate and constant rpm.
- iii. To determine the AST power output and the highest efficiency based on three external and internal AST design parameters.

1.4 Scopes of the Study

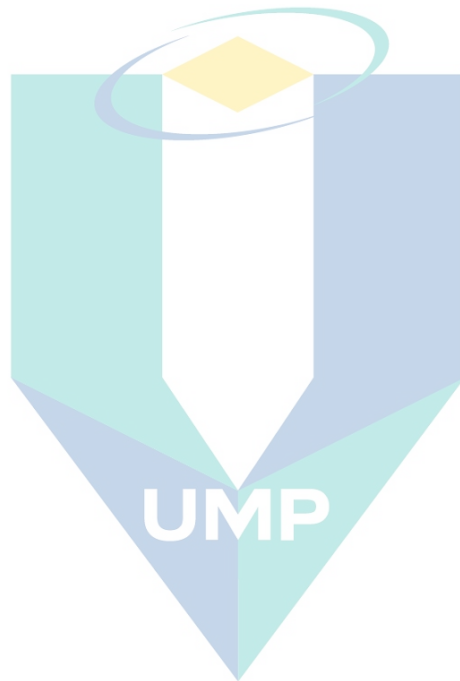
- i. This study focused on power production of AST using two internal (number of bladed screws and diameter ratio) parameters and one external (slope inclination angle) parameter.
- ii. The blade length, inner diameter, outer diameter, pitch, and slope inclination angle of the AST model were drawn according to the dimensions of a previous

- study (0.646 m, 0.032 m, 0.142 m, 0.054 m, and 30°, respectively). These design parameters were obtained from Erinofiardi et al., (2017).
- iii. The geometry was drawn using the Solidworks software, with two parts (the stationary part and the blade part) for each of the design criteria.
 - iv. ANSYS CFX software was used to simulate the AST model.
 - v. Mesh sensitivity analysis was used to validate the numerical and experimental data compared between five mesh sizes, with a constant water flow rate (1.2kg/s), angle of inclination (30°), and 146RPM of rotational speed. The lowest percentage error, 5.95% (with 500,000 nodes), is chosen to proceed with the other simulation using the independent parameters.
 - vi. The inlet, outlet, and wall boundary conditions were assumed to be constant. In this simulation setup, the rotational speed is set up manually based on the value in the previous experiment by Erinofiardi et al. (2017). Basically, the AST blade is rotating when the water enters the turbine, but due to software set up limitations, in this research, the rotational speed is set up in the setting part.
 - vii. The simulation was done using three independent parameters (i.e., the diameter ratio of 0.25, 0.5, and 0.6; the slope inclination angle of 20°, 25°, 35°, and 40°; and the number of blades of 1–3 bladed screws).
 - viii. The power output is calculated from the torque generated from the simulation, while the efficiency depends on the power output and input of the AST.

1.5 Summary

This thesis is divided into five chapters: Introduction; Literature Review; Methodology; Results and Discussion; and Conclusion and Recommendations. Chapter 1 presents a brief explanation of the RE produced from hydro power using the AST, problem statement, and discusses the objectives and scope of this research. The thesis structure is described at the end of this chapter. A short overview of the literature relevant to the research study is given in Chapter 2. The main goal of this review is to gain a better understanding of AST studies. The overview is focused on hydropower energy, the types of parameters in AST, and the method used to obtain the performance of AST studies. Chapter 3 presents the methods used (numerical) to meet the objectives, as specified in Chapter 1. Chapter 4 reports the results and analysis of the results to support the

objectives. Finally, Chapter 5 provides the conclusion and recommendations for improvement in future studies.



اونيورسيتي ملايسيا قهغ

UNIVERSITI MALAYSIA PAHANG

CHAPTER 2

LITERATURE REVIEW

2.1 Introduction

The purpose of this chapter is to briefly describe the background and prior findings of the related studies, which cover the type of renewable energy (RE), the history of the Archimedes screw, parametric studies of the Archimedes screw turbine (AST), and methods used to determine the power output and efficiency of the AST. This chapter also discusses the analysis of computational fluid dynamics (CFD) in simulating the flow of the AST, where the numerical simulation is validated with the experimental results in the aspects of power output generated by the AST. The data in this chapter comes mostly from other researchers' results that are relevant to the current project.

2.2 Renewable Energy

Malaysia's demand for energy consumption is increasing due to the country's rapid development. To avoid current energy demand shortfalls, RE is seen as a solution to this problem because RE can be replenished at the same rate as it is used. Several commonly used sources of RE are solar, biomass, biogas, municipal solid waste, hydro, fuel cells, wind, and geothermal power (Baños et al., 2011; Borhanazad et al., 2013; Ong et al., 2011). Figure 2.1 shows Malaysia's primary energy consumption in 2011 for crude oil (i.e., vehicle fuel) (31%), natural gas (28%), coal (24%), crude oil (14%), and hydro power (3%) (H. Y. Chong & Lam, 2013). Hydro power is not utilised wisely where hydro power is a substantial source of electrical energy compared to fossil fuels and nuclear fuels.

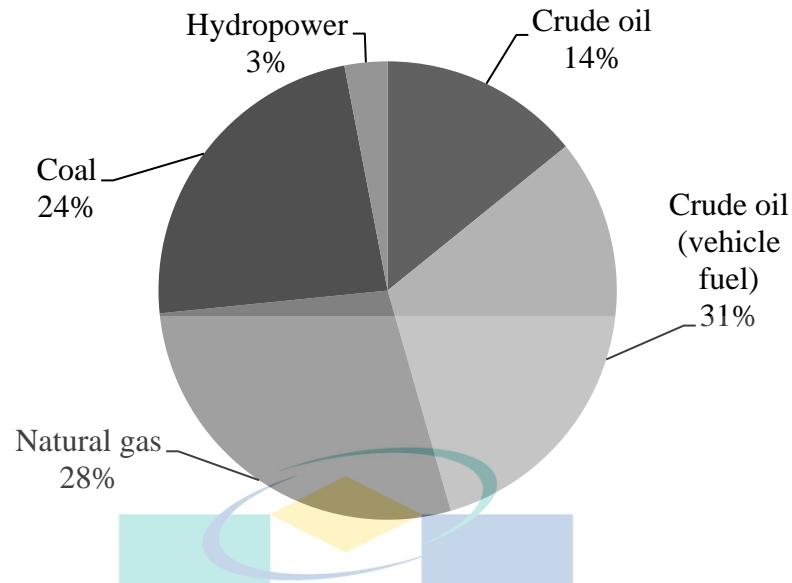


Figure 2.1 Malaysia's primary energy consumption in 2011

Source: H. Y. Chong & Lam (2013)

Generally, about 71% of the Earth's surface is covered by water; hence, hydro power can be one of the best solutions to generate energy from water. Several methods for generating energy from water sources include tidal waves, ocean waves, and hydro power. Hydro power can be classified into five categories in terms of the power output, such as large, small, mini, micro, and pico hydro power. Figure 2.2 lists the classifications of hydropower plants. A large hydropower plant can achieve more than 1,000 kW of electricity. The power range for a small hydropower plant is 500–1,000 kW, whereas a mini hydropower plant has a capacity of between 100 and 500 kW, and a micro hydropower plant can have an output power of between 5 and 100 kW (Mohibullah et al., 2004). The output of a micro hydropower plant can be used in rural areas, specifically for small or medium houses.

In Malaysia, the development of hydro power is expected to increase from 5% to 35% in 2030. The largest hydropower plant in Malaysia is located in Sarawak (Bakun Dam, which has a capacity of 2,400 MW), followed by Murum Dam (940 MW), Baleh Dam (950 MW), and Pelagus Dam (770 MW) (Ong et al., 2011). However, these hydropower plants require large areas as they are categorised as impoundment hydropower plants. Another two features of hydropower plants are diversion and run-of-river. A run-of-river hydropower plant uses a natural flow range and requires small a

reservoir; thus, this type of plant only needs a small space. Meanwhile, a diversion hydropower plant may not need to use dams. An impoundment hydropower plant is a large hydropower system that uses a dam to store river water (i.e., needs a large area) and the stored water is then used to generate electricity (Keawsuntia, 2014).

Table 2.1 Classification of hydropower plants

Classification of Hydropower Plants	Output Power Generated
Large	More than 1,000 kW
Small	500–1,000 kW
Mini	100–500 kW
Micro	5–100 kW
Pico	< 5kW

Source: Mohibullah et al., (2004)

2.3 Hydropower Plant

Hydro power is a form of energy derived from water sources for generating electricity. Due to the increasing demand for electricity supply, hydro power is one of the solutions. The concept of hydro power means the energy from falling water is converted into electrical energy using a power converter, such as a turbine. The turbine will act as a converter of the falling water energy (kinetic energy) into mechanical energy. Then, a generator is used to convert the mechanical energy into electrical energy, as shown in Figure 2.2. In terms of advantages, several aspects are considered when installing this type of power. Hydro power has low maintenance and operating costs (economic aspect), can use free and available natural water (social aspect), and can simultaneously reduce climate change and increase the water ecosystem.

Mohibullah et al. (2004) discussed the conceptual design and development of a micro hydropower plant in Malaysia, which is expected to have a 50 kW power plant. The aspects that should be considered when developing a plant are the measurements of head and flow, civil work components, selection of the turbine, hydrology and site survey, drive systems, and electrical power. All of these should be considered as factors affecting the performance of the power generated (Mohibullah et al., 2004). Nasir (2014) presented

a paper that used Simulink MATLAB for calculating all the design parameters for a micro hydropower plant, and stated that the choice of the appropriate turbine used was influenced by the head and flow rate at the site. Besides, the varied flow rate also affected turbine power and speed. The range of efficiency achieved was 80%–95%. Figure 2.3 illustrates the schematic diagram of a micro hydroelectric power plant.

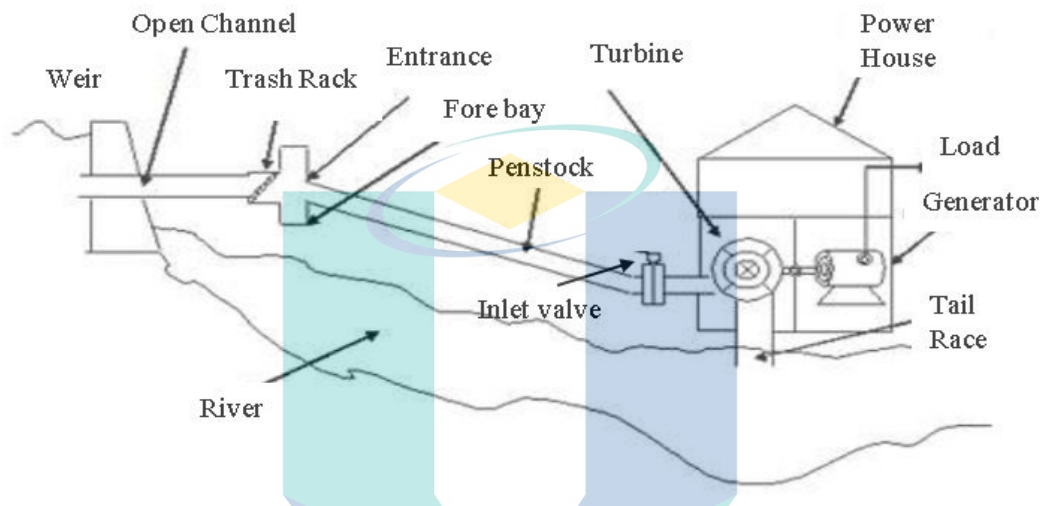


Figure 2.2 Schematic diagram of a micro hydroelectric power plant

Source: Nasir (2013)

The design factors covered in the research are the flow duration curve, flow rate measurement, weir open channel, trash rack design, head measurement, turbine power, turbine speed, and turbine selection (Nasir, 2014). The results from the simulation showed that the gross head at varied water flow rates is directly proportional to the turbine power and speed, whereas the flow rate at different values of gross head is directly proportional to the speed and power of the turbine, which would achieve a maximum value at specific points.

2.4 Archimedes Screw Runner Blade

2.4.1 History of the Archimedes Screw Runner Blade as a Pump and Turbine

The designing of the Archimedes screw pump was done circa 250 BC and became one of the technologies many years ago. The first function of this technology was to lift water for irrigation and drainage (Rorres, 2000; Stergiopoulou et al., 2013). As presented

in Figure 2.3, the water allocated from the bottom reservoir is transferred to the top side of the reservoir by rotating the screw blade. The water is trapped between the flight and will enter the blade while rotating (Lubitz et al., 2014; Rorres, 2000). This type of pump is selected due to its simplicity, easy handling, durability, and safety to aquatic life.

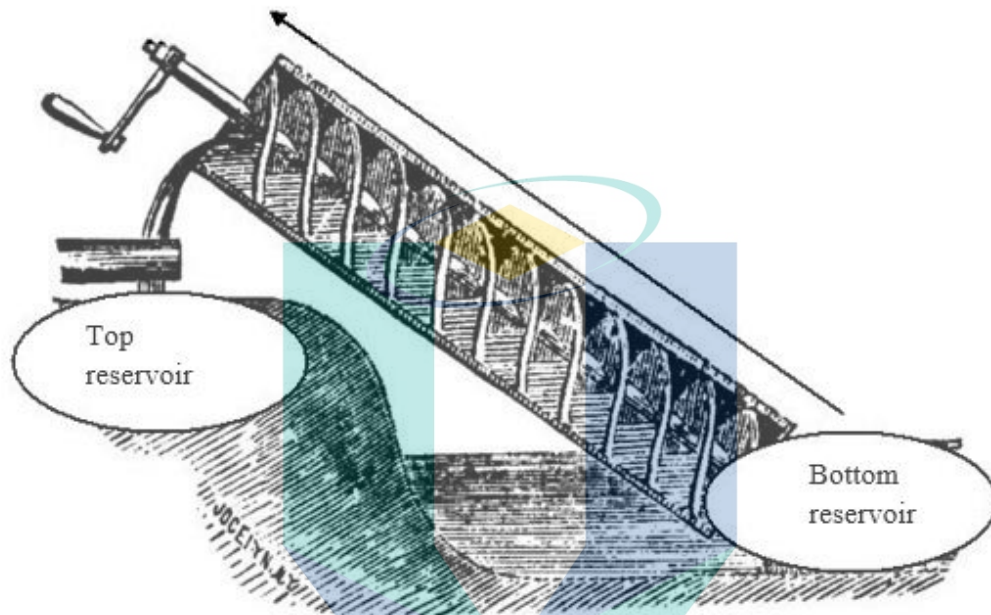


Figure 2.3 A three-bladed Archimedes screw runner pump
Source: Rorres (2000)

As technology has rapidly changed, the innovation of the Archimedes screw pump has been developed in a reverse direction. As illustrated in Figure 2.4, the Archimedes screw blade is used as a turbine to generate energy. The turbine works in a different direction from the pump as the former has a reverse function (Muller & Senior, 2009; Rorres, 2000). The head difference that exists at the level of water is different between the top and bottom reservoirs. The water flows from the top reservoir and forms a bucket, which makes the blade rotate along the length of the Archimedes screw blade (Lubitz et al., 2014). Meanwhile, the inclination of blades forms a hydrostatic force, where the downstream pressure acting on the blade is smaller compared to the upstream level (Muller & Senior, 2009). Due to the hydrostatic force, the blade rotates to produce kinetic energy, and the turbine turns a generator rotor. Lastly, electrical energy is generated.

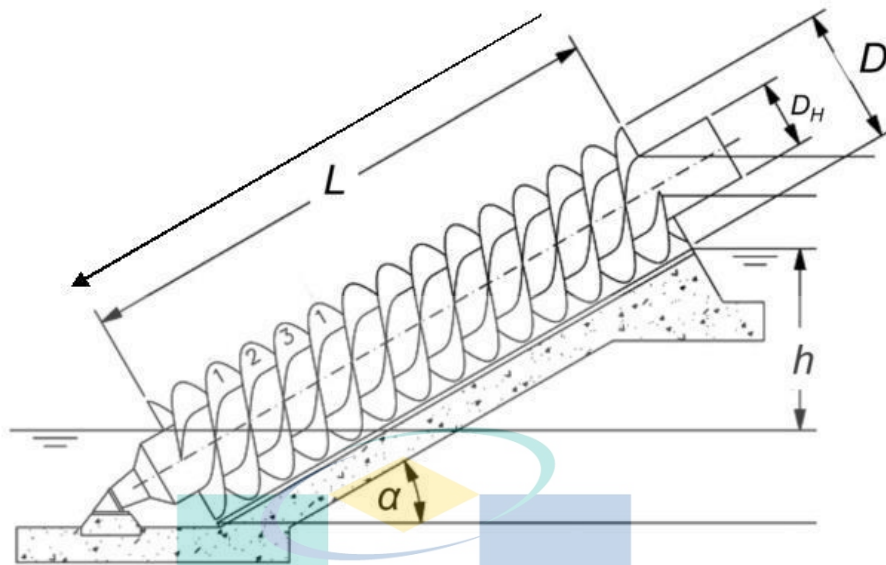


Figure 2.4 Side view of the Archimedes screw turbine
Source: Muller & Senior (2009)

2.4.2 Advantages of the Archimedes Screw Turbine

The turbines usually used for hydropower purposes can be classified into impulse and reaction turbines. Both turbines work differently; an impulse turbine does not need a pressure difference for the water to move the blade, whereas a reaction turbine requires a pressure difference to make the runner rotate (L. Barelli, L. Liucci, A. Ottaviano, 2013). The AST is classified as a reaction turbine. Figure 2.5 explains the graph of hydro power for the head versus water flow rate. The head difference is the main criterion for categorising hydropower turbines. A suitable turbine for a micro hydropower plant should be less than 10 m. The AST has 10 m of head and less than $10 \text{ m}^3/\text{s}$ of flow rate. Meanwhile, the AST offers advantages in many aspects, which are high stability, economical, accomplished by generating reliable energy needed, requiring minimal civil works, and having low environmental impacts (Date & Akbarzadeh, 2009; Elbatran et al., 2015; L. Barelli, L. Liucci, A. Ottaviano, 2013; Lubitz et al., 2014; Lyons & Lubitz, 2013; Shimomura & Takano, 2013).

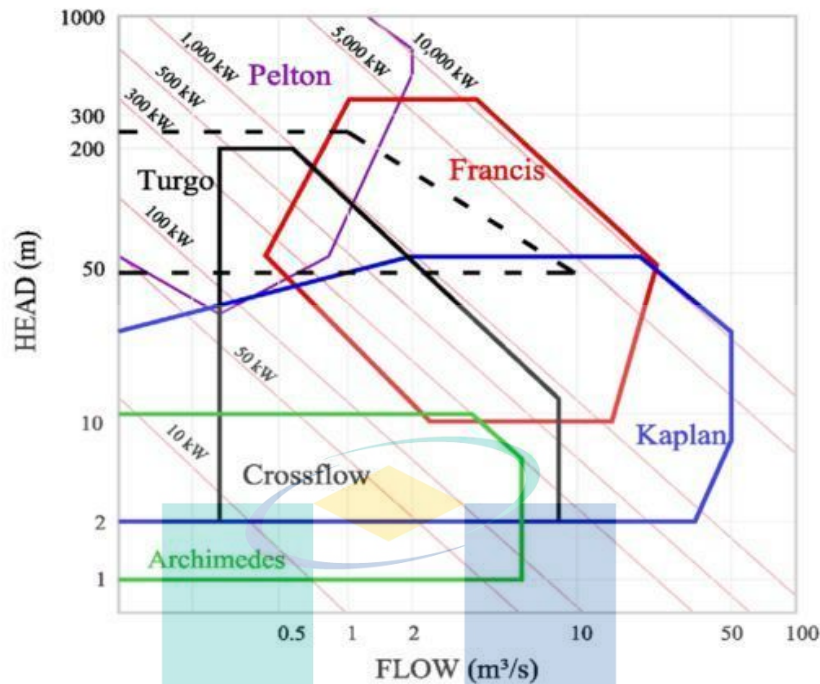


Figure 2.5 Classification of head and water flow rates for different types of turbines
 Source: L.Barelli, L. Liucci, A. Ottaviano (2013)

2.4.3 Concept of Archimedes Screw Turbine Application

The AST is classified as a reaction turbine, where the turbine needs a pressure difference to rotate the blade (L. Barelli, L. Liucci, and A. Ottaviano, 2013). The AST is more efficient at high flow rates and lower heads. From Figure 2.5, it is clearly shown that the AST has a range of head from 1 to 10 m compared to other turbines; thus, the AST is suitable to be implemented due to the power output generated, especially in a rural area. The main concept of the AST energy conversion, where the water that falls from the gravitational force contributes to potential energy. As the water hits the blade, the blade starts to rotate (kinetic energy) and the rotation turns the generator rotor (mechanical energy), thus leading to electrical energy production (refer to Figure 2.6).

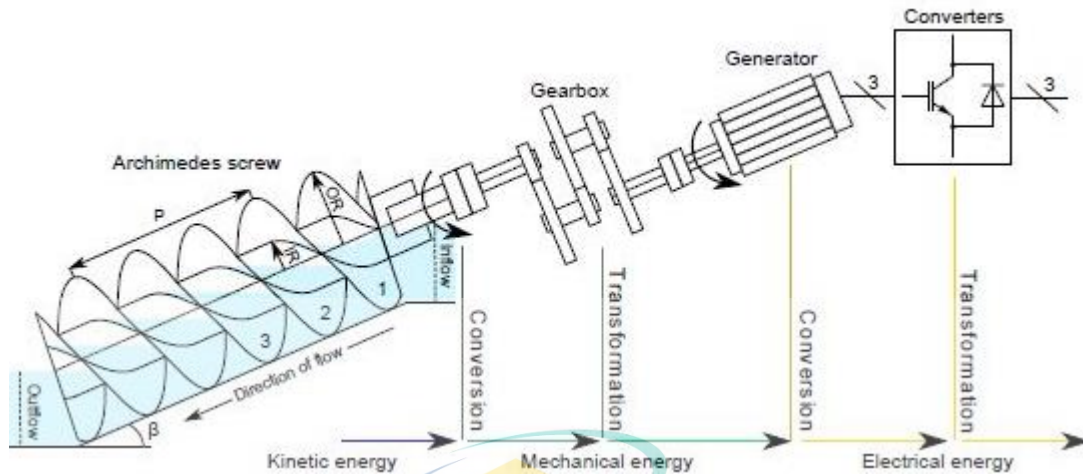


Figure 2.6 Energy conversion of Archimedes Screw Turbine (AST)

Source: Rohmer et al., (2016)

Previous studies reported that the efficiency of a turbine could reach 100% by assuming no losses (Muller & Senior, 2009). However, most cases of turbine applications have weaknesses that will reduce turbine efficiency. In the AST, the screw blade static at the trough affects turbine efficiency. The gap losses are ignored in most studies. Based on Figure 2.7, the head difference, length of the screw blade, and number of turns have a significant relationship with water.

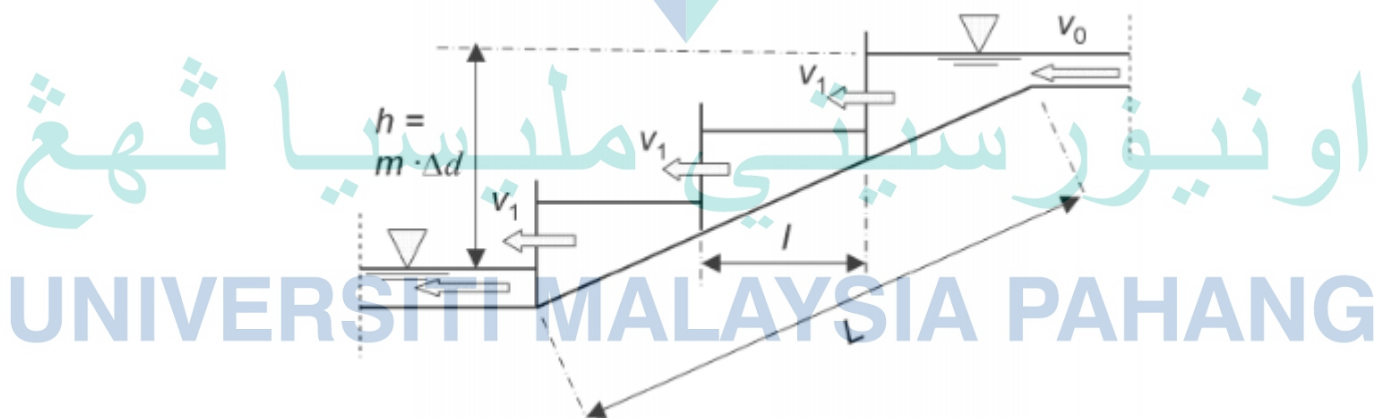


Figure 2.7 Side view of the AST diagram

Source: Muller & Senior (2009)

Several parameters need to be considered when designing a screw for a specific site, such as the screw inner diameter, outer diameter, screw pitch, number of flights, overall length, and slope angle. Hydraulic force, F_{hyd} is generated when the water level is different between the up and down streams. Moving at a screw speed, v_1 will generate power, P_{blade} as expressed in Equation 2.1:

$$P_{blade} = F_{hyd} \times v_1 \quad 2.1$$

With the angle being relatively horizontal to the distance between two individual blades, the water depth increases by Δd , as shown in Equation 2.2, where h is the head difference, m is the number of turns, α is the slope inclination angle, L is the length of the screw:

$$\Delta d = \frac{h}{m} = l \tan \alpha = \frac{L}{m} \tan \alpha \quad 2.2$$

The hydrostatic force can be calculated using Equation. 2.3, where d_0 is the inflow depth, ρ is the density, and g is the gravity:

$$F_{hyd} = \frac{(d_0 + \Delta d) - d_0^2}{2} \rho \cdot g \quad 2.3$$

The approach flow velocity, v_1 is then expressed in Equation 2.4:

$$v_1 = \frac{d_0}{d_0 + \Delta d} \cdot v_0 \quad 2.4$$

With m blade, the total power becomes $P = mP_{blade}$ and the available P_{hyd} is shown in Equation 2.5, where Q is the flow rate:

$$P_{blade} = \rho \cdot g \cdot Q \cdot H = \rho \cdot g \cdot d_0 \cdot v_0 \cdot m \cdot \Delta d \quad 2.5$$

The theoretical efficiency, η_{th} can be calculated using Equation 2.6:

$$\eta_{th} = \frac{d_0}{\Delta d} = \frac{2n+1}{2n+2} \quad 2.6$$

Where $\eta_{th} = d_0/\Delta d$ and $\eta_{th \min} = 0.5$ for the case of $n \rightarrow 0$ or $d_0 \rightarrow 0$.

2.5 Parameter Studied for AST

Detailed analysis of AST parameters is provided in this section. According to Table 2.2, three common methods are used: experimental, simulation, and numerical. In general, past researchers have employed the experimental technique. However, the numerical technique was used in this research study to determine the AST's power production and efficiency. Previously, in terms of parameters studies, the impact of the gearing system, slope inclination angle, flow rate, number of bladed screws, number of helixes turns, rotational speed, length of the blade, head difference, and volume of water were explored by researchers.

On the basis of AST geometric characteristics, several models have been created to design and optimise performance. The slope inclination angle is the most commonly studied characteristic. The average slope inclination angle used is in between a minimum of 10° and a maximum of 50°. Kashyap et al., (2020) experimentally investigated the effect of slope inclination angle between 20° and 50° and had a maximum efficiency of 70%, 49%, and 61.61% at 20°, 22°, and 35°, respectively. Meanwhile, the maximum power output generated was at 45° (0.00915kW), 40° (1.4W), and 35° (16.23W), which differed from the maximum efficiency angle value.

Abdullah et al., (2021) used two different methods, numerically and experimentally, using the physical model to determine the performance of AST. The angle of investigation was set at 30° to 45°, and achieved a maximum efficiency of 80% at 35° and a maximum AST power of 25.13W at an angle of 45°. However, the results are different from the study made by Shahverdi et al., (2020), which used the same numerical method. 20kW power output with 90.83% efficiency can be generated by using a 20° slope inclination angle. It can be concluded that only several researchers achieved the

maximum efficiency and power output from the AST with the same slope inclination angle.

In addition, other than the numerical and experimental methods used previously, studies based on simulation have also been considered (Dellinger et al., 2019). By using boundary conditions that are close to experimental, the data is validated by comparing it with the results from the experimental study. The best efficiency (86%) occurred at 24.5°, while the achieved optimum power output (38.147W) was at 33°.

Maulana & Putra, (2019) investigated whether the gearing system has any impact on the power performance of AST. Two models of AST were experimentally designed with gear and no gear usage. The gearbox was able to boost the AST rotation from 236 rpm to 567.46 rpm during the Archimedes single-blade turbine rotation experiment. With a flow rate of 0.05 m³/s, an acquisition power of 15.38 W, and a final rotation of 410.67 rpm, the best turbine performance utilising gear transmission was achieved. It can be said that the gearing system also has an impact on the AST power output. Additionally, the rotational speed of AST depends on the turbine design, as once the model achieves its optimum level of rotational speed, the performance of power output will start to decline.

Due to the complexity of the experimental fabrication of the AST-bladed screw, the majority of studies use a single-bladed screw for the AST-bladed screw parameters. Zafirah Rosly et al., (2016) analysed the impact of the bladed screws on the efficiency of the turbine. Based on the results of the study, it was found that an optimum efficiency of 91% was achieved when a 3-bladed screw (with 3 helix numbers) was adapted. Meanwhile, the efficiency of the 2-bladed screws decreased by 30%. The effect of the three different numbers of blades (3, 4, and 5) of an AST with common design parameters was then simulated using CFD (Dellinger et al., 2019). At higher inclinations, overflow and gap leakage losses increased. However, these losses decreased with the addition of blades. The 5-bladed screw produced the maximum power in this AST configuration. At inclination angles of 20° to 24.5°, the 4- and 5-bladed screws had the highest efficiency. The 3-bladed screw was discovered to have the best efficiency at comparably lower inclination angles, with an optimum angle of around 15.5°.


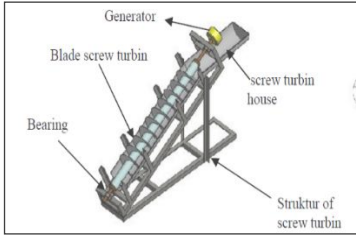
The fluid flow code in ANSYS was used to assess the performance of parameters with changing numbers of blades, and the result showed the highest efficiency of 87% with a 5-bladed screw compared to the lowest efficiency of 21% using a 10-bladed screw. By increasing the number of blades, pressure is created at its highest impact at the start of the turbine's blades, which is not spread evenly along the blade's length. The majority of the water will spill over or overflow, reducing the amount of effective torque.

Numerically, Shahverdi et al., (2020) found that a 1-bladed screw resulted in an efficiency of 90% compared to a 5-bladed screw that had the lowest efficiency of 62.8%. and 3-bladed screw is enough to obtain an 81.4% efficiency due to the difference between torque values, which decreases as the blade size increases. The optimal number of blades may be selected as the manufacturing process gets more difficult and costly as the number of blades increases.

The effect of various angles and average discharge was experimentally investigated by Embangkit et al., (2012). The researchers concluded that both parameters affected the performance of the Archimedes turbine. The efficiency is optimum at an angle of 35° at the highest average discharge. Meanwhile, another experimental method was performed by considering the volume of water and head height with respect to the rotation of the screw blade. It was found that rotation is directly proportional to the volume of water and the head (Hendra, 2014).

In another study, (Borhanazad et al., 2013) investigated the relationship between the inflow head and turbine axis angle that varied with water velocity and slope inclination angle, and observed that the highest efficiency was achieved at the high inflow head, high water velocity, and low slope inclination angle. However, the relationship between the turbine axis angle and the rotation rate is explained in terms of the rotation rate, where high rotational speed is achieved at a high turbine axis angle. Lubitz, (2014) concluded that the screw turbine will operate sufficiently when the volume of buckets is nearly filled, but cannot be overfilled at moderate operating speeds, while the gap leakage should be considered as it will influence the efficiency.

Table 2.2 Summary of parameters studied by previous researcher

Researcher	AST Design	Methods	Parameter studies	Results
Effect of flow discharge and shaft slope of Archimedes (Screw) Turbine on the Micro Hydro Power plant (2012)		Experimental	Flow rate between 0.00364 m ³ /s to 0.00684 m ³ /s. Slope inclination angle between 25° to 50°	Optimum AST power and efficiency at flow rate 0.00684m ³ /s, slope inclination angle of 35 (with 16.231 W of power output and efficiency of 61.61%)
Manufacture of Screw Turbine and Placement of the Generator in the Screw Turbine Shaft Used for Small-scale of Micro Hydro Electrical Generating (2014)		Experimental	Head difference: 450mm, 550mm and 650mm. Water Volumes: 19L and 100L	Maximum AST rotation (330RPM) at 650mm head difference with 100L water volume

اونیورسیتی ملیسیا قهنگ

Table 2.2 Continued

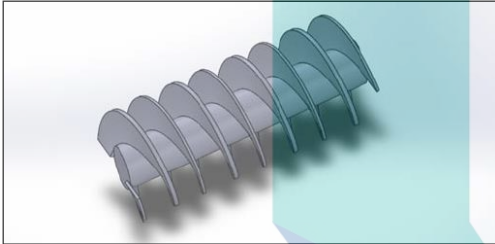
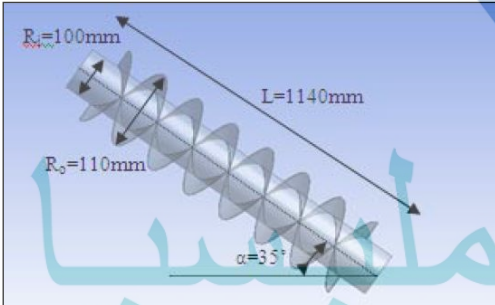
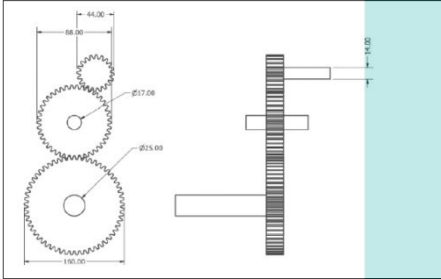
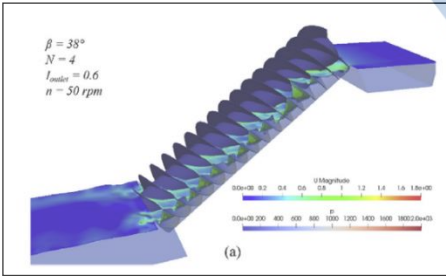
Researcher	AST Design	Methods	Parameter studies	Results
A Theoretical Study of Design Parameters of an Archimedean Screw Turbine (2015)		Theoretical	2 number of bladed screws	By using the calculation, the efficiency achieved 69.76% with 1.25 rev/s Each bladed screw has different optimal radius ratio, optimal pitch ratio, optimal volume per turn ratio and optimal volume ratio
Parametric study on efficiency of Archimedes Screw Turbine (2016)		Simulation	Number of bladed screws= 2 and 3 Helix number= 3, 6 and 9	For 2-bladed, maximum efficiency 61% at 3 helix For 3-bladed, maximum efficiency 91% at 3 helix

Table 2.2 Continued

Researcher	AST Design	Methods	Parameter studies	Results
Performance of single screw Archimedes turbine using transmission (2019)		Experimental	2 gear transmission: have gear and not have gear system 2 flow rates: 0.05 m ³ /s and 0.0375 m ³ /s	Design with gear have better power performance, than have no gearing system. Rotational speed and loads impact the power output of AST.
Effect of slope and number of blades on Archimedes screw generator power output (2019)		Simulation	Slope inclination angle: between 10° and 38° Number of bladed screw: 3,4, and 5	Generated most power: 5-bladed screw (38.147W) 4- to 5-bladed screws have the highest efficiency between 20° and 24.5° (85% to 86%) 3-bladed screw has the best efficiency (85%) at 15.5° slope inclination angle

اونيورسيتي ملايسيا قهق

Table 2.2 Continued

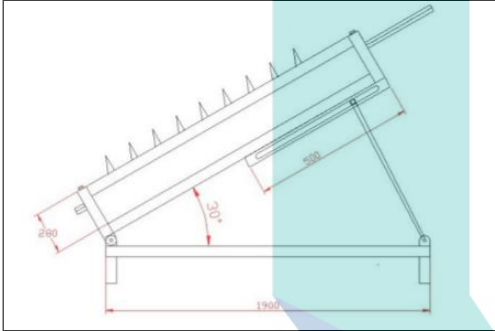
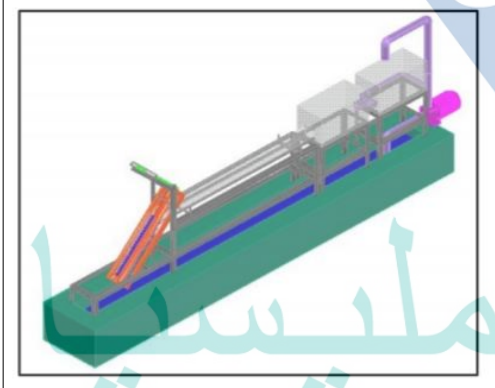
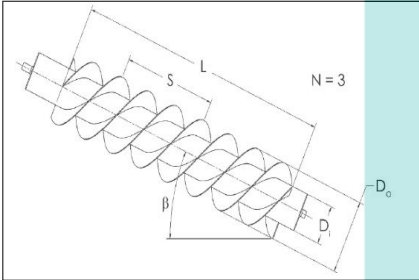

Researcher	AST Design	Methods	Parameter studies	Results
Design and Performance of Archimedes Single Screw Turbine as Micro Hydro Power Plant with Flow Rate Debit Variations (Case Study in Air Dingin, Samadua - South Aceh) (2019)		Experimental	Flow rate: 0.02m ³ /s, 0.009 m ³ /s, 0.003m ³ /s	Highest rotation, power and efficiency is 236.40 RPM, 116.10W, 57% respectively at 0.02 m ³ /s.
Experimental Study: The Influence of Shaft Slope on Rotation of the Three Bladed Archimedes Screw Turbine (2018)		Experimental	Slope inclination angle= 10°, 20° and 30°	Maximum turbine rotation achieved 416 RPM ($\alpha=30^\circ$) Minimum turbine rotation achieved at 250 RPM ($\alpha=10^\circ$)

Table 2.2 Continued

Researcher	AST Design	Methods	Parameter studies	Results
A power loss model for Archimedes screw generators (2017)		Experimental		The primary source of power loss is due to AST outlet submerge level.
Numerical and experimental study of an Archimedean Screw Generator (2016)		Numerical and experimental	Slope inclination angle: 18° to 30° Flow rate: 0.001 to 0.004 m ³ /s Rotational speed: 60 RPM to 180 RPM	At flow rate 0.002 m ³ /s with 70 RPM rotational speed, the screw operates in over-filling

اونیورسیتی ملیسیا پاهانغ

UNIVERSITI MALAYSIA PAHANG

Table 2.2 Continued

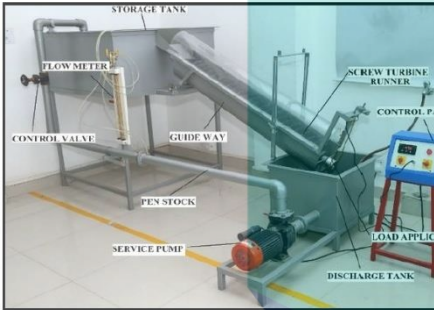

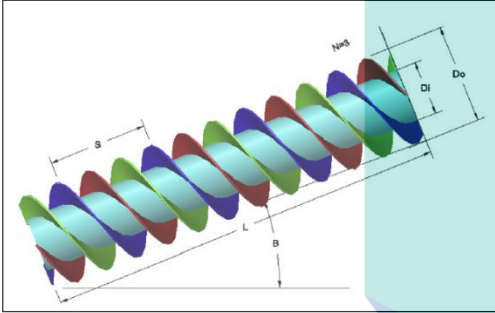
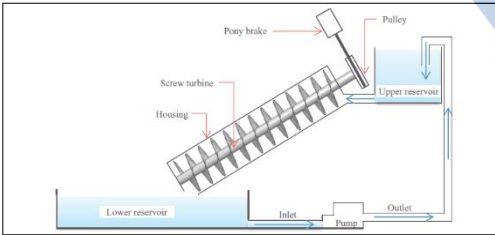
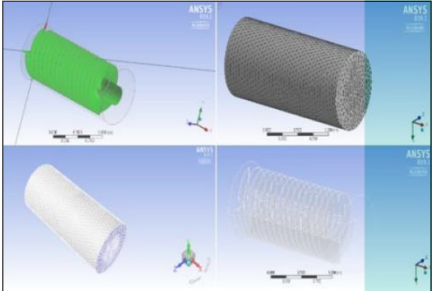
Researcher	AST Design	Methods	Parameter studies	Results
Identification of Archimedes Screw Turbine for Efficient Conversion of Traditional Water Mills (Gharats) into Micro Hydro-power Stations in Western Himalayan Regions of India: An Experimental Analysis (2020)		Experimental	Slope inclination angle: 20° to 50 °. Flow rate: 1 to 4 L/s. Pitch: 0.1, 0.2 and 0.3m	Maximum efficiency at 70%, with slope inclination angle of 20° and 1.0 L/s flow rate.
Numerical and experimental modelling of small hydropower turbine (2020)		Numerical and experimental	Slope inclination angle: 30° to 45° Flow rate: 0.75 L/s to 2.5 L/s Number of bladed screw: 1–6	Highest efficiency: 81.4%, slope inclination angle of 35° and flow rate of 1.12 L/s. Highest power 25.13W obtained at 45° with flow rate of 2.065 L/s (efficiency at 72%).

Table 2.2 Continued

Researcher	AST Design	Methods	Parameter studies	Results
Numerical Optimization Study of Archimedes Screw Turbine (AST): A case study (2020)		Numerical	Slope inclination angle: 15° to 30° Length: 4m to 7m Number of bladed screw: 1-5	With 1 number of bladed screw, the efficiency is optimum at 20° to 25° for blade lengths of 4m to 7m. Highest efficiency (90%) at 20° slope inclination angle at 1 bladed screw with 6m length.
Experimental study of screw turbine performance based on different angle of inclination (2017)		Experimental	Slope inclination angle: 22°, 30° and 40°	Maximum efficiency=49% with 22°, and 1.4W power output Maximum power at 1.4W at 22° and 40°.

اونیورسیتی ملیسیا قہنگ

Table 2.2 Continued

Researcher	AST Design	Methods	Parameter studies	Results
Investigation of Archimedean Screw Turbine for Optimal Power Output by Varying Number of Blades (2019)		Simulation	Number of bladed screw: 1–10 Diameter ratio: 0.54	Efficiency: highest (87%) with 5-bladed screw Efficiency: lowest (21%) with 10-bladed screw The highest efficiency at 5-bladed screw (87%), with 3.29 Nm torque and 12.58kW power output.

UMP

اونيورسيتي ملايسيا قهق

UNIVERSITI MALAYSIA PAHANG

Based on the previous research study, this chapter identifies numerous gaps that could be addressed in this study to highlight the major factors that influenced the AST's power output and efficiency. The combination of internal and external parameters should be considered when determining the best AST design. As a result, the relationship between slope inclination angle, number of bladed screws, and diameter ratio is investigated. Most researchers conclude that 1–5 bladed screws are more efficient, so the number of bladed screws chosen was between 1 and 3, because 4 and 5 bladed screws are more expensive to manufacture. Meanwhile, previous researchers' common diameter ratio was between 0.5 and 0.6, but one study used 0.25Dr as a case study, so the Dr of 0.25, 0.5, and 0.6 was chosen to identify the effects on power production and AST efficiency. According to previous research, a low inclination angle leads to increased efficiency and vice versa. As a result, the low and high slope inclination angles are used to compare the relationship between a wide range of slope inclination angles, diameter ratios, and the number of bladed screws.

Thus, the AST's design parameters will be 20° to 40° slope inclination angle, 0.25 to 0.6 diameter ratio, and 1 to 3 bladed screw. Prior to this study, researchers did not combine all three parameters. As a result, all three parameters are examined in this research study.

2.6 Computational Fluid Dynamics (CFD)

One of the best approaches to optimising design parameters is by using computational fluid dynamics (CFD) simulation. The method offers many benefits to researchers and design engineers. For example, the actual flow pattern can be seen clearly through simulation compared to the experimental method. Moreover, CFD is an effective and cost-saving tool for predicting the actual flow, and further enhancement can be done using this tool (Prasad et al., 2009). The results from this research indicate that the results from the numerical simulation are quite similar to the experimental results. The difference may be due to errors in numerical simulation caused by the discretisation of the domain and differential equations. Meanwhile, experimental studies are affected by human errors during the experimental setup.

Wang et al. (2012) investigated the design of an axial water turbine with the combination of a nozzle, wheel, and diffuser. An analysis of three-dimensional numerical flow and flow characteristics was performed. Using this method, torque and power can be generated using different rotational speeds. For a given flow rate, the extracted power and torque of a composite water turbine were measured and evaluated at different rotational speeds. The results show that the pressure drop increased with the use of a nozzle and diffuser, hence resulting in more power generation from the water energy. These findings show a clear understanding of a water turbine by just using simulation.

The study of the AST using ANSYS CFD was carried out by Maulana et al. (2018) to predict the effect of screw number using only a one-bladed screw. The results were tabulated in the form of a pressure analysis. Furthermore, this method was also used by Khan et al. (2019) to identify the power output of the AST in terms of pressure, torque, mechanical power, and efficiency. Hence, it can be concluded that ANSYS CFX simulation is one of the best methods to identify the flow pattern, pressure analysis, torque, mechanical power, and efficiencies without conducting experiments that may have cost constraints.

The Navier Stokes equations of a conventional turbulence model are solved to investigate the structure of 3D turbulent flows and energy losses in a screw. As shown, the strength of this technique is that it allows for reliable analysis of ASG performance using just standard coefficients in turbulent closure models (Dellinger et al., 2018). Numerical simulations were conducted to determine the turbine's performance coefficient (without frictional losses or blockage augmentation) and to increase the top speed ratio range. Further, Khan et al., (2019) presents a Computational Fluid Dynamics (CFD) study of a 3-D model numerical simulation of a stable turbulent water flow through an Archimedes screw turbine.

The fluid flow in CFD is based on the governing equations used, including continuity, Navier-Stokes, and energy equations. The three physical laws adopted are:

- i. Conservation of mass (continuity equation);
- ii. Conservation of momentum (Navier-Stokes equation); and
- iii. Conservation of energy.

Most cases in engineering applications involve turbulent flow. It is difficult to simulate the flow as turbulence is unsteady and three-dimensional (3D). Hence, three approaches have been introduced to computationally identify turbulent flow: direct numerical simulation (DNS); large eddy simulation (LES); and Reynolds-averaged Navier-Stokes (RANS) methodology.

The conservation of mass or the continuity equation states that the mass cannot be created or destroyed. The integral equation of continuity is presented in Equation 2.7:

$$\frac{\partial \rho}{\partial t} + \frac{\partial(\rho u)}{\partial x} + \frac{\partial(\rho v)}{\partial y} + \frac{\partial(\rho w)}{\partial z} = 0 \quad 2.7$$

The conservation of momentum is derived from Newton's second law, where the sum of external forces acting on a moving system is equal to the rate of change of the system's momentum. The flow field is defined in three components (u, v, and w) or in general forms (x, y, and z components).

The integral equations of momentum conservation for x, y, and z directions are shown in Equation 2.8, Equation 2.9, and Equation 2.10, respectively:

$$\rho \frac{Du}{Dt} = \frac{\partial \sigma_{xx}}{\partial x} + \frac{\partial \tau_{yz}}{\partial y} + \frac{\partial \tau_{zx}}{\partial z} + \sum F_x^{bodyforce} \quad 2.8$$

$$\rho \frac{Dv}{Dt} = \frac{\partial \sigma_{xy}}{\partial x} + \frac{\partial \tau_{yy}}{\partial y} + \frac{\partial \tau_{zy}}{\partial z} + \sum F_y^{bodyforce} \quad 2.9$$

$$\rho \frac{Dw}{Dt} = \frac{\partial \sigma_{xz}}{\partial x} + \frac{\partial \tau_{yx}}{\partial y} + \frac{\partial \tau_{zz}}{\partial z} + \sum F_z^{bodyforce} \quad 2.10$$

CHAPTER 3

METHODOLOGY

3.1 Introduction

This chapter discusses the methodology used in this study, which consists of data validation with experimental work by a previous researcher. Following the validation of the experimental and numerical data, three additional AST models were created by varying the geometric parameters (i.e., slope inclination angle, α ; diameter ratio, D_r ; and number of bladed screws, N). Then, the models were simulated using ANSYS CFX by applying the boundary conditions, and the results of the simulation were presented in the form of torque. Further discussions on the methodology are presented in the following subchapter.

Figure 3.1 shows the overall flow chart used in this research to ensure that the objectives of the research can be achieved. The details and steps for conducting the simulation are discussed and explained. External (α) and internal parameters (D_r and N) were chosen in this study. Several steps need to be completed for a successful simulation. The steps include constructing the geometry of the AST model, meshing, checking the quality of the mesh, linking both rotating and stationary domains, applying the boundary conditions in ANSYS CFX, and finally, running the simulation. The tolerance or convergence criteria should be checked to ensure that the simulation converged and the torque data was collected from the post-processing results. In the ANSYS CFX simulation, the value of torque will be used to figure out how much power and how efficient the AST will be.

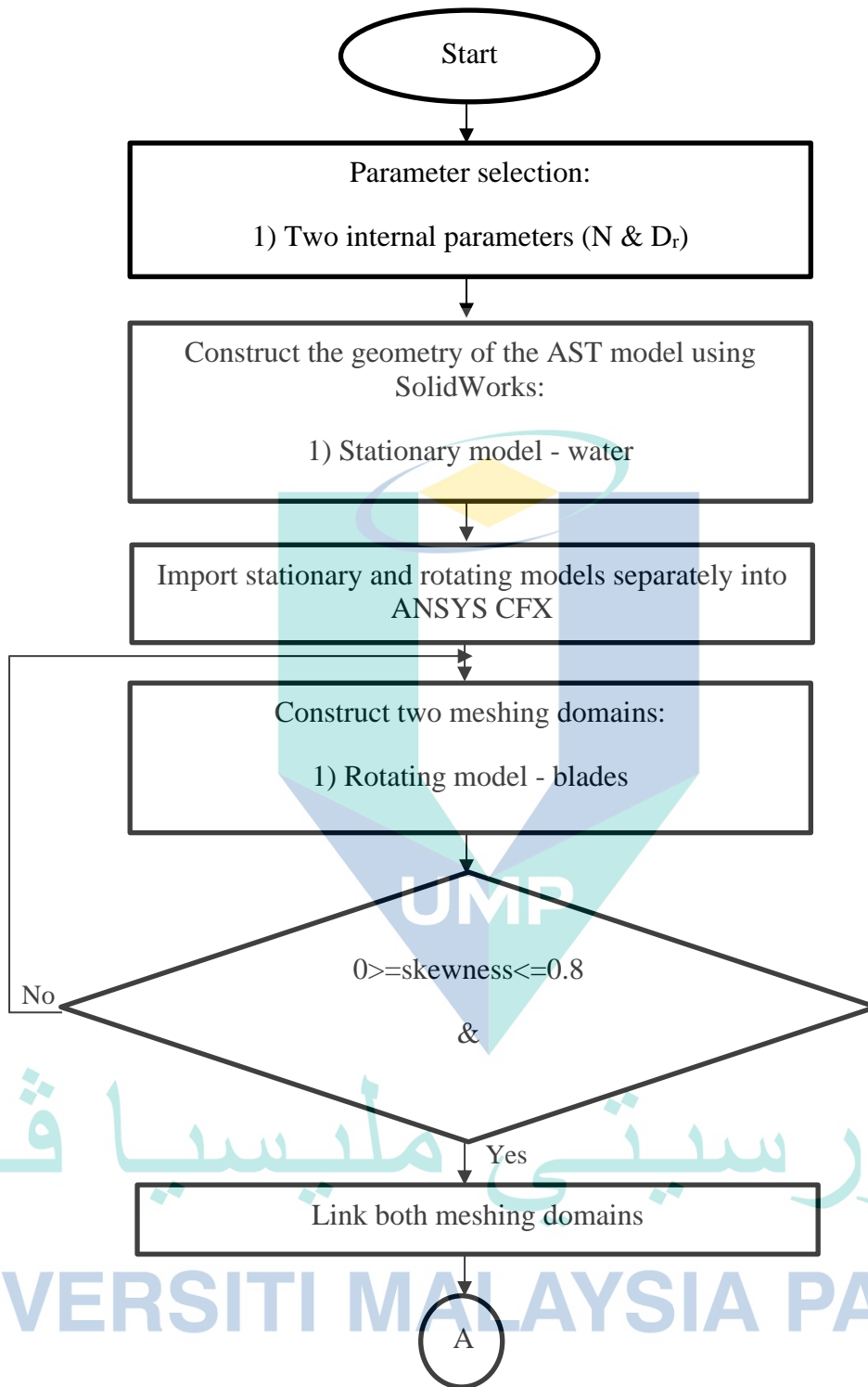


Figure 3.1 Research flow chart

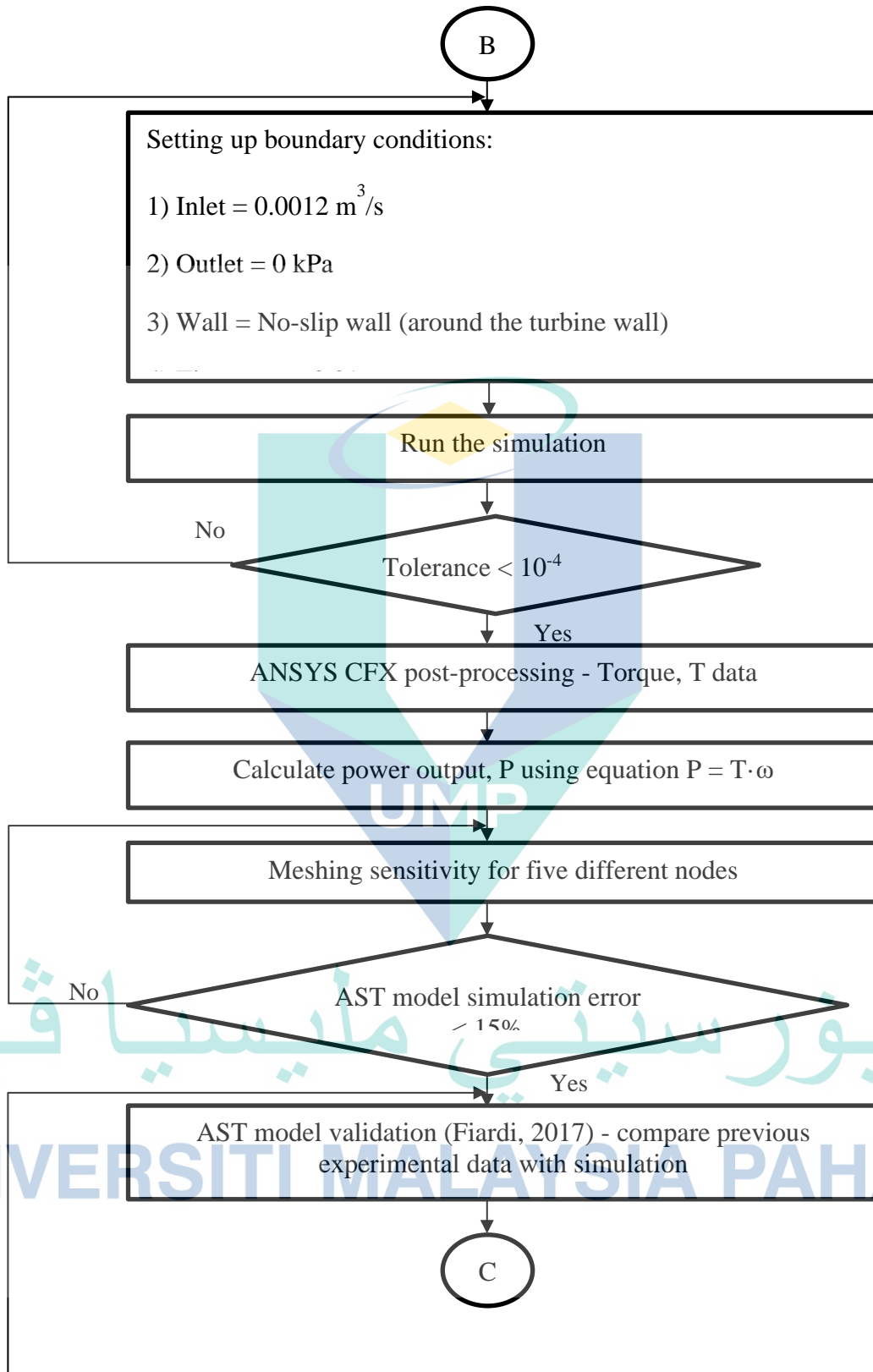


Figure 3.1 Continued

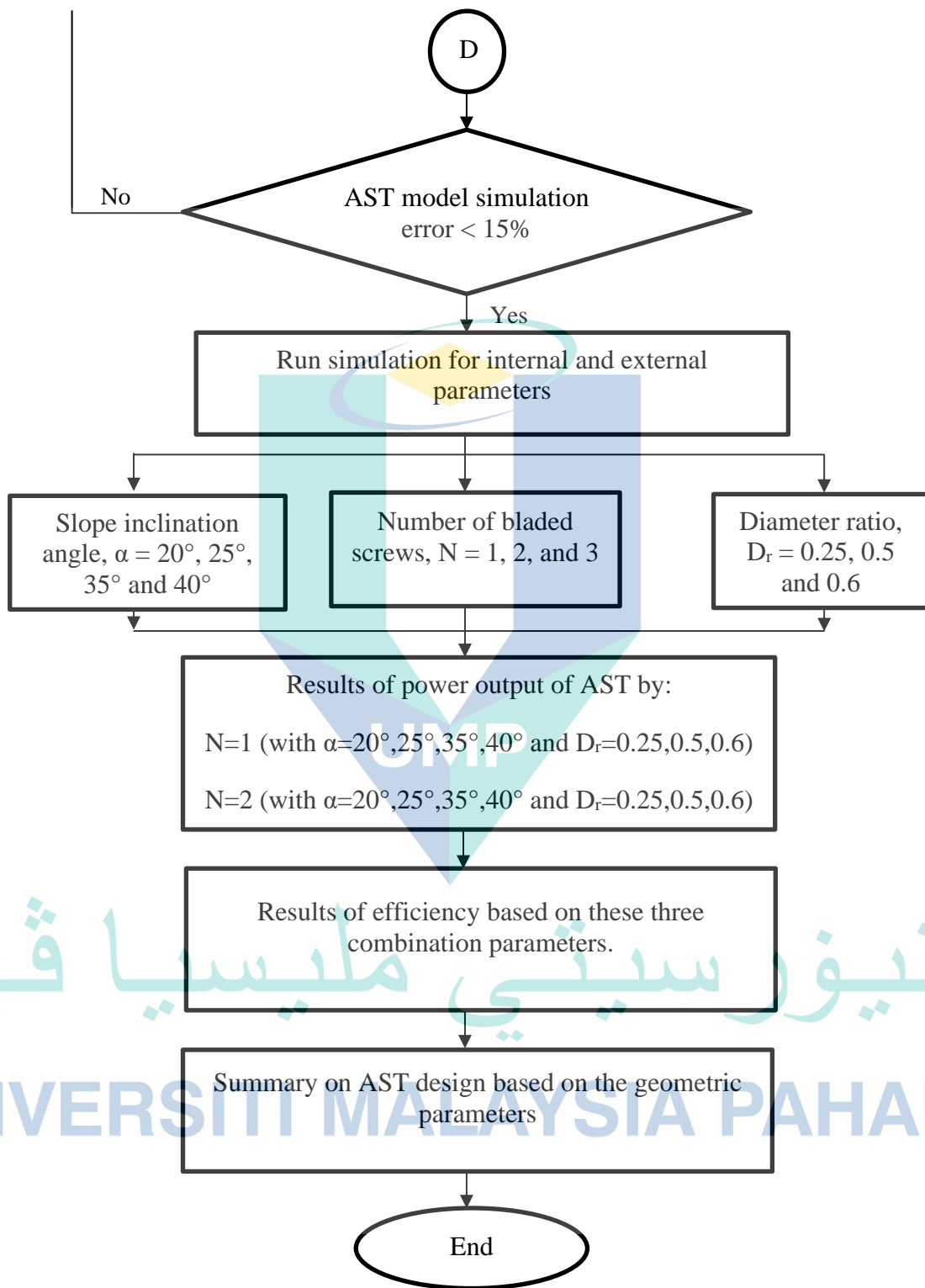


Figure 3.1 Continued

Several researchers have studied the AST; hence, several parameters were selected in this study. One external (α) and two internal parameters (N and D_r) were chosen. First, the geometric model of the AST was drawn using computer-aided design (CAD) software, namely SolidWorks 2019, and saved in the IGS format. Two types of models were drawn: stationary (flow) and rotating (AST blade) models. Then, the flow and blade of the AST geometric models were imported separately for the meshing step using ANSYS CFX. The models were meshed into stationary and rotating AST domains. However, the geometric models need to be reviewed and the mesh setting needs to be set up again if an error occurs during meshing, such as one or more entities failing to mesh, the surface mesh intersects or is close to intersecting, or the mesh could not be generated using the current meshing option and setting. Once the meshing step was successful, both models were connected using the interface setting. Besides, the meshing metrics also need to be checked. For example, the skewness and orthogonal quality should be close to 0 and 1, respectively. Acceptable skewness is in the range of 0–0.8, and the orthogonal quality is between 0.2 and 1.0. Subsequently, both domains were linked.

The boundary conditions were applied based on real experimental conditions. The inlet, outlet, wall, time step, volume fraction, iteration, and model types were applied accordingly. The simulation was conducted after all the boundary conditions were set up. If there was no error and the simulation ran smoothly and converged, the simulation could proceed. However, if the simulation encounters errors, then the setup of boundary conditions must be reviewed and redone.

After the simulation ran smoothly and converged, the results of torque were collected from the ANSYS post-processing data. The power output and efficiency of the AST were calculated. Details of the calculation and equation will be discussed in Subchapter 3.5. Torque was obtained from the simulation results, and ω was taken from the setup of the earlier data. The simulation was repeated five times to complete the mesh sensitivity, where the simulation error should be less than 15%. Then, the AST model validation of Erinofardi et al. (2017) was compared with the simulation output. If the results of the experiment and the simulation were in line, the simulation would be kept running with other variables that could be changed, like (external) and N and D_r (internal).

The torque generated results from the simulation were collected from the post-processing of ANSYS CFX. The results are presented in terms of power output, which can be calculated. The simulation results were collected and analysed in terms of power output and efficiency. A total of 36 simulations were conducted for $\alpha = 20^\circ, 25^\circ, 30^\circ$ and 40° , $N=1,2,3$ and $D_r=0.25,0.5$ and 0.6 . All parameter values were simplified and selected based on the previous study (Erinofiardi et al., 2017) . The results of the power output of AST will be presented in three sections, such as at $N=1$, $N=2$, and $N=3$ with various slope inclination angles and diameter ratios. Meanwhile, for efficiency, the results will be averaged across all 36 simulations. Lastly, from the generated results, the conclusion is based on the impacted parameters on the AST design.

3.2 Simulation of Parameter Selection

Several geometric parameters were selected and investigated to determine the power output of the AST. Each parameter affects the power output of a turbine significantly. In this study, the geometric parameters are the properties of the AST, where the combination of parameters would affect power production. Figure 3.2 shows the geometrical parameters of the AST. The listed geometrical parameters affect the flow characteristics and hydrodynamic force within the turbine. Based on a previous study, the dimensions of the model are shown in Table 3.1.

اونيورسيتي ملايسيا قهغ

UNIVERSITI MALAYSIA PAHANG

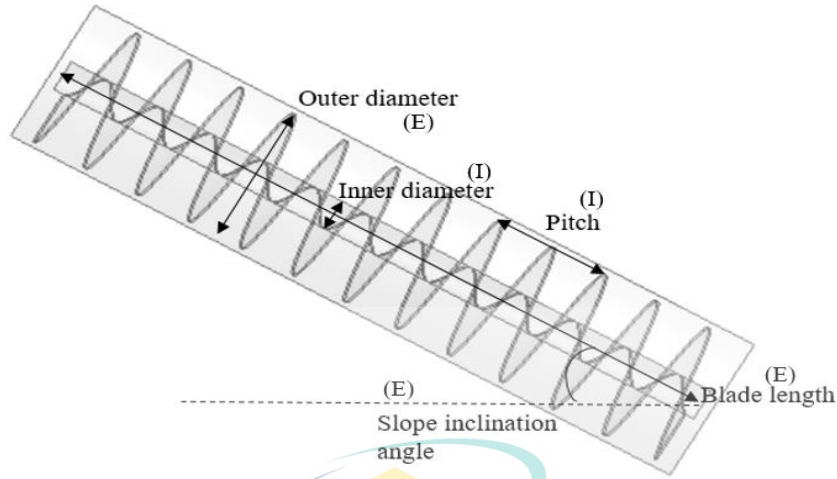


Figure 3.2 Geometrical parameters of the AST model

Table 3.1 Dimensions of the AST model Erinofiardi et al., (2017)

Geometry	Dimension
Blade length	0.646 m
Inner diameter	0.32 m
Outer diameter	0.142 m
Pitch	0.054 m
Slope inclination angle	30°

3.2.1 Independent Parameter

Three geometric parameters were investigated in this study to determine the AST power and efficiency generated from this model. Each parameter has its own effects at a different level. Three parameters were studied (i.e., α , D_r , and N). All these parameters influence the flow characteristics and hydrodynamic force of the AST. The range of α , D_r , and N for the simulation study is summarised in Table 3.2. These parameters can be classified into internal and external parameters.

Table 3.2 Geometric parameters for the simulation study

Geometric Parameters	Specifications
α	20°, 25°, 35°, and 40°
D_r	1, 2, and 3
N	0.25, 0.5, and 0.5

3.2.2 Internal Parameters

Three internal parameters were considered for the AST model: the number of bladed screws, inner diameter, and pitch of the blade. The details of the parameters are shown in Figure 3.2. Internal parameters are usually used to optimise screw performance. The letter “I” indicates internal parameters.

3.2.3 External Parameters

The external parameters act as the controlled parameters of the turbine and water flow (outer diameter, length of the screw, and slope inclination angle), as shown in Figure 3.2. The letter “E” indicates external parameters.

3.3 Dimensional Analysis

Dimensional analysis is one of the important factors in the study of transforming a unit from one form into another, also known as unit conversion. Three basic quantities of a dimensional system are mass, m; length, l; and time, t, with the units of kg, m, and s, respectively. The basic definition of dimensions means only that quantities with similar dimensions can be added or subtracted. If the quantities have similar dimensions, then two physical quantities are identical.

The dimensional analysis in this study was performed to determine the significant independent parameters affecting the power generation. Two internal parameters and one external parameter were considered as the geometric AST parameters for generating torque with the relationship of power, $P = T \cdot w$.

The dimensional analysis of the power output of the AST was considered. The equation of power includes multiplying the torque applied to the shaft and rotational speed. The calculation of the dimensional parameters is shown as follows:

$$P = T \cdot \omega$$

Where $T = F \cdot r$

$$F = \frac{[m][l]}{[t]^2} \text{ and } r = [m]$$

Where $F = \text{kg} \cdot \text{m/s}^2$ and $r = \text{m}$.

From the experimental values of the previous researcher:

$$P_{\text{exp}} = 1.3 \text{ W}$$

$$P_{\text{theory}} = 4.3 \text{ W}$$

$$\omega = 15 \text{ rad/s}$$

$$\alpha = 30^\circ$$

$$T = 0.09 \text{ Nm or } T = 0.09 \text{ kg} \cdot \text{m}^2/\text{s}^2$$

Where $1 \text{ Nm} = 1 \text{ kg} \cdot \text{m}^2/\text{s}^2$.

The calculation to change the unit of rad/s to degree is as follows:

For $\omega = 15 \text{ rad/s}$ and $t = 0.01 \text{ s}$,

$$15 \text{ rad/s} = 15 \text{ rad/s} \times 360/2\pi \times 0.01 \text{ s} = 8.59^\circ$$

Hence, from the calculation above, the value α that suits 15 rad/s or 146 rpm of the experimental study is equal to 8.59° . As the power equation depends on the rotational speed and the torque exerted on the shaft, it can be concluded that the rotational speed depends on α , which is related to the head difference of the blades. Meanwhile, the torque generated depends more on the values of N and D_r of the AST.

3.4 Computational Fluid Dynamics Simulation

In this section, the CFD methodology was used to model the fluid flow within the AST. The AST model was simulated using ANSYS CFX to calculate the torque and

power output generated. In this simulation, the incompressible, multiphase, and turbulent flow conditions were applied. First, the numerical results were studied and validated using the experimental results of (Erinofiardi et al., 2017). Once the data was validated, the simulation using other parameters (α , n , and D_r) of the screw blades was analysed to obtain the results of power output and efficiency based on the number of bladed screws, $N=1, 2$, and 3 .

3.4.1 Simulation Set Up

3.4.1.1 Ansys CFX Simulation Environment

ANSYS CFX version 16.2 was used to simulate the fluid flow of the AST. Three main elements should be prepared in setting up this simulation, such as the pre-processor, processor, and post-processor, as illustrated in Figure 3.3.



Figure 3.3 Schematic diagram of CFD elements

Source: Tu et al., (2018)

Details of the simulation step are indicated in Figure 3.4 below. The blade and flow are meshed separately by stationary and rotating domains. Then, in the post-processing part, both the blade and flow parts are combined using the interface to connect and reattach both domains. All the boundary conditions set up are done at the post-processing part, followed by the solution by running the simulation.

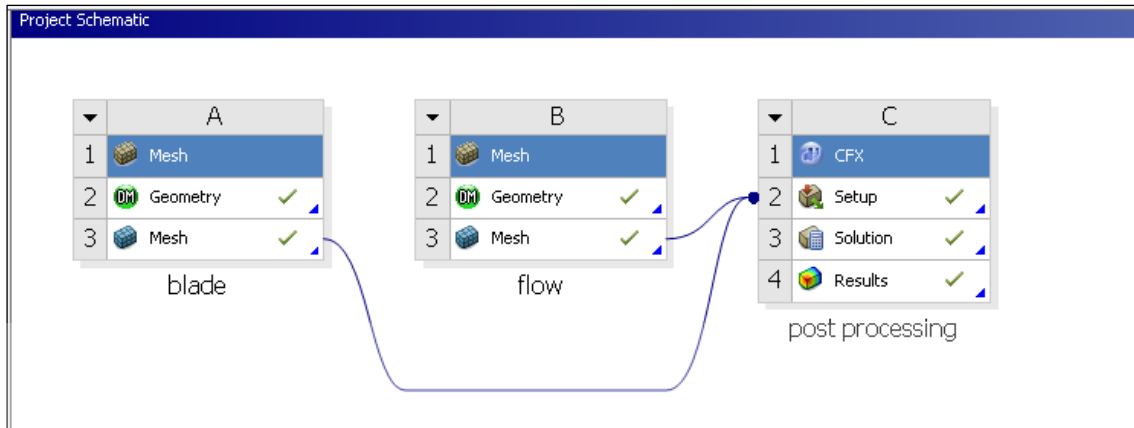


Figure 3.4 Details project schematic using ANSYS CFX

The first step in this CFD method is to determine the geometry of the stationary and rotating domains. The file will be imported into the geometry part of ANSYS CFX. The second step is to choose the type of mesh (i.e., coarse, medium, or fine). The size of the mesh will affect the node and element numbers of the geometry model. The third step is the selection of physics and fluid properties. Appropriate flow physics should be carefully selected in order to simulate fluid flow characteristics. The boundary conditions should be chosen properly to determine the fluid behaviour when entering and leaving the domain flow. Lastly, the simulation is started and checked for convergence. If the results converge to the desired tolerance that has been set, then the simulation is completed. In case the simulation does not converge well, some modifications should be made where the boundary conditions should be checked in the processor step. The results in terms of torque can be collected from the post-processing element.

3.4.1.2 Geometry and Meshing Generation

The AST model was created using SolidWorks 2019. The dimension of the screw is similar to the experimental geometry of the previous study by Erinofiardi et al., (2017). In this study, two parts of geometry were created: the blade (rotating) and flow (stationary) parts. The screw inclination angle was set at 30° with a gap of 0.001 m. For all simulations, a constant gap of 0.001 m was chosen as this gap is the maximum hydraulic loss by leakage. The dimensions of the geometry are shown in Table 3.1. Figure 3.5 indicates the flow part, whereas Figure 3.6 indicates the blade part. The geometry of the fluid entering the turbine was created using the extruded boss and extruded cut

techniques. Meanwhile, for the blade part, the extruded boss, extruded cut, and swept cut options were used. Both geometries were then saved in the IGS format file so that they could be used with ANSYS Design Modeller.

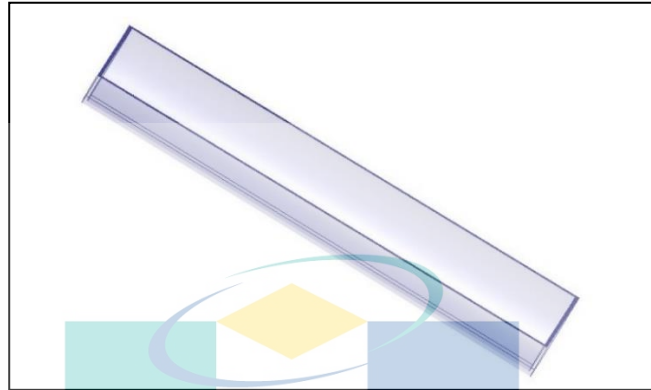


Figure 3.5 Cross section - stationary part of the flow

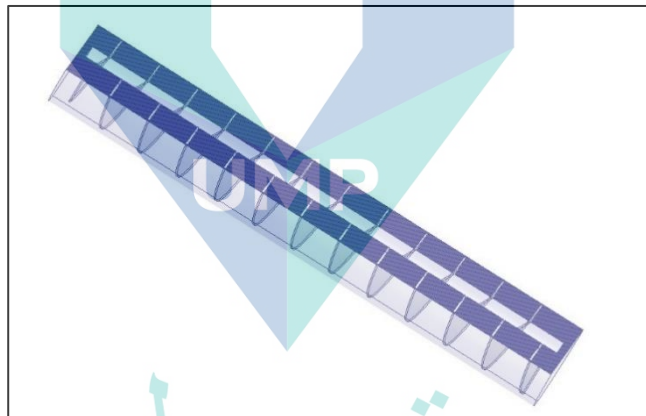


Figure 3.6 Cross section - rotating part of the blades

As shown in Figure 3.7, the combination of rotating and stationary elements means the inlet is located on top, and the outlet is located on the bottom. Basically, in this simulation, water is set up to enter the AST at 30% and 70% of air, which can be adjusted in the setup step. This assumption is critical because, in practice, water cannot enter the AST completely because only a small part of the water enclosed in the screw contributes to energy conversion. Besides, due to some limitations, the rotational speed is set up earlier using the CFX-Preprocessing step. Due to simulation setup during the validation, it was decided to simulate the AST at a constant flow rate of $0.0012\text{m}^3/\text{s}$ and a constant

rotating speed of 146RPM. The actual and modelled torque values are very similar at 30% water and 70% air. Basically, the water flow rate and the rotational speed are linked together to make sure that the loss of torque during torque generation is kept to a minimum. Meanwhile, a prior study by Dellinger et al., (2019) used 60% water and 40% air, which is slightly different due to the study's use of variable water flow rates ranging from 0.006 m³/s to 0.012 m³/s with a constant flow rate of 60 RPM.

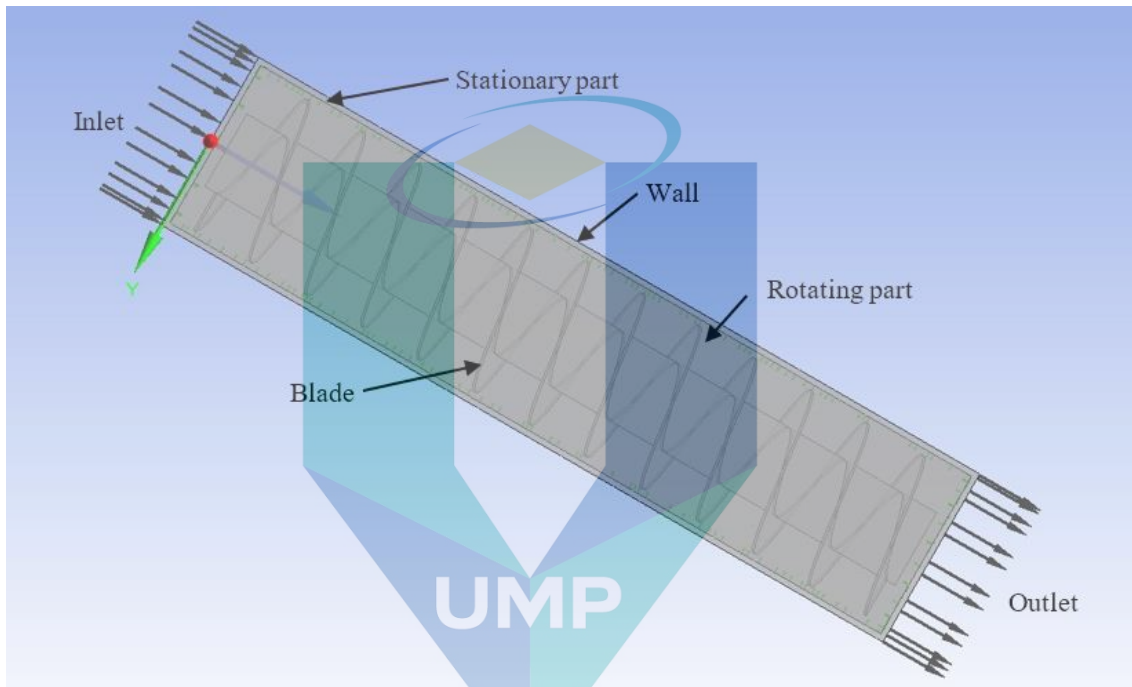


Figure 3.7 Boundary condition applied

For the finite volume method (FVM), the pattern of discrete points is known as a grid or mesh, and the method is suitable for unstructured mesh (Manoj Kumar Shukla, Prof Vishnu Prasad, 2011). Three important and useful elements to obtain precise results are convergence, stability, and consistency.

UNIVERSITI MALAYSIA PAHANG

$$\int_V \frac{\partial u}{\partial t} + \int_V \nabla \cdot f(u) dV = 0 \quad 3.1$$

Where f corresponds to the flux tensor. By integrating the volume that contains a divergence term to obtain a volume average, this equation yields:

$$V \frac{\partial u}{\partial t} + \int_A f(u) \cdot n dA = 0$$

Where A is the total surface area of the control volume (CV) and n is a unit vector normal to surface. The terms are evaluated as fluxes at the surface of each CV.

The type of element classification for 3D elements can be divided into four basic shapes: tetrahedra, hexahedra, pyramid, and triangle. Meanwhile, the method of meshing consists of tetrahedrons, hex dominant, and sweep and multi-zone methods. As shown in Figure 3.8, the relevance centre can be modified into coarse, medium, and fine meshes. The accuracy of the result increases for smaller mesh. Sensitivity analysis can be done to test the accuracy of the results, depending on the mesh.

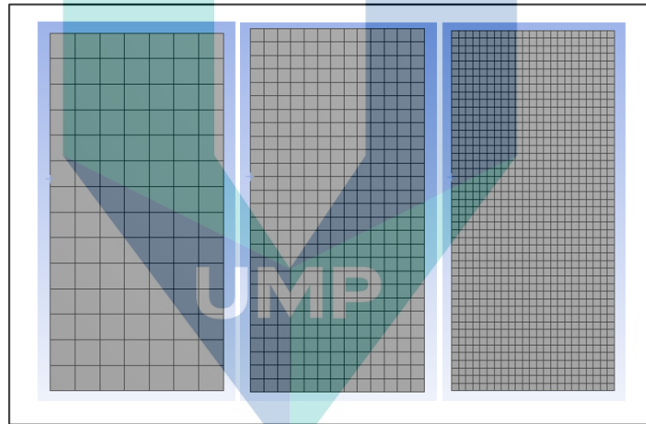


Figure 3.8 Coarse, medium, and fine relevance center of meshing

In this study, two parts of geometry were mesh separately (i.e., the flow and blade parts). Both parts were meshed using the tetrahedral method, which can fit well with complex geometry. The computational meshing needs to be built carefully to ensure the result is stable and realistic.

Figure 3.9 and Figure 3.10 show the meshing of the blade parts, where the fluid part was meshed instead of the blade itself.

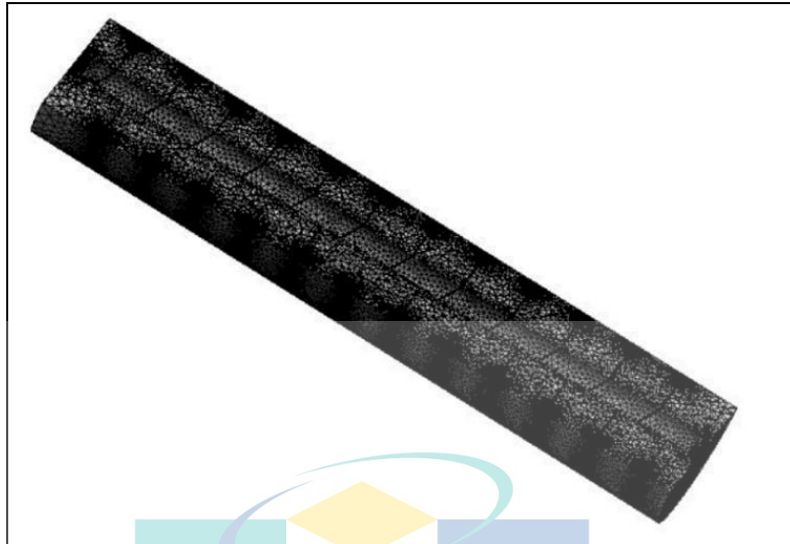


Figure 3.9 Meshing of blade part

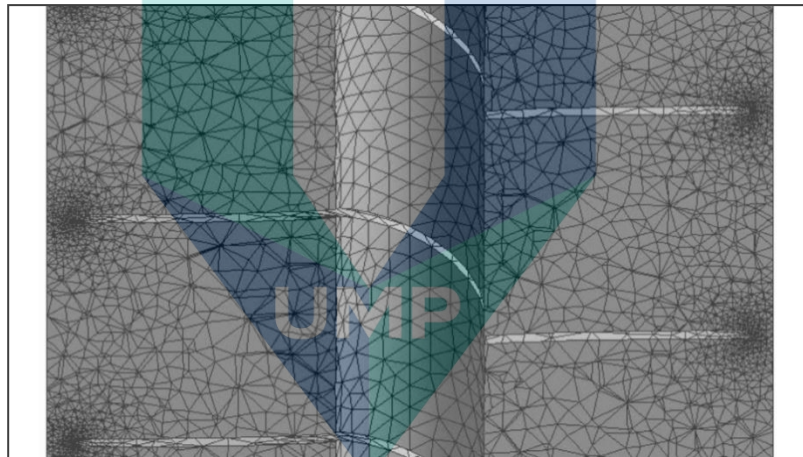


Figure 3.10 Close up of the meshing of blade part

For the meshing part, the validation of meshing parameters in simulation is important to ensure the results generated are accurate, acceptable, and significant. In ANSYS CFX, there are several aspects considered, such as aspect ratio, orthogonal, skewness, and Jacobian ratio. All of these aspects have their own level to achieve the highest accuracy in results. Table 3.3 indicates the type of quality level of the results. In this study, the skewness and orthogonal quality are checked.

Table 3.3 Type of quality and the level of accuracy

Type of quality	Specification
Aspect ratio	0 to 1, approaching 1 is the best
Orthogonal	0 to 1, approaching 1 is the best
Skewness	1 to 0, approaching 0 is the best
Jacobian ratio	-1 to +1, approaching +1 is the best

Skewness is defined as the difference between the shape of an equilateral cell of equivalent volume and an unshaped cell. Basically, the maximum skewness of the mesh in flow should be kept below 0.95, with an average value that is less than 0.33. In this study, the maximum skewness is 0.8 and the average skewness is 0.24 with a 0.77 orthogonal quality value; both are acceptable for the meshing requirements.

3.4.1.3 Boundary Conditions

Boundary conditions are significantly important in numerical simulation (Munson et al., 2013). The numerical simulation in this study consists of two domains: the rotating and stationary parts. In the rotating domain, the empty blade part was chosen as the blade will rotate when water enters the turbine (i.e., the rotating domain consists of a blade and a trough). The volume of fraction (VOF) method was used in this simulation as the model consists of 30% water and 70% air as its domain. Eventually, the rotational speed of the rotating domain is equal to the rotational speed of the screw turbine blade. The rotating blade domain was included in this simulation by using a rotating frame of reference. Meanwhile, for the stationary part, the fluid domain was set as water and air entered the turbine. Two types of domains were considered (i.e., a combination of two different types of fluid). Figure 3.7 indicates the set up for boundary conditions used in this study.

Each domain is essential as it has its own significant effect. In this study, three boundary domain conditions were applied: the inlet, outlet, and wall. The water flow rate entering the turbine was controlled by the inlet boundary, whereas the outlet boundary controlled the water leaving the turbine. The wall condition was applied around the wall turbine. A no-slip wall was applied at the water wall due to the existence of viscosity, where the velocity at the wall point is zero, which is suggested on all the rigid walls. Furthermore, the interface method was used to ensure the connection between the

domains (i.e., stationary and rotating domains) using the frame change model of the frozen rotor type. After all, if there are no boundary conditions applied, the software will detect the default settings, which may lead to inaccurate results due to the different conditions with the experimental setup needed. For this simulation, the fluid was assumed to be isothermal and incompressible flow, which has a constant temperature and fluid density. The computational simulation was conducted under transient conditions with a time step of 0.01 s.

3.4.1.4 Governing Equation

The fluid flow was analysed by considering three fundamental equations in CFD. They are the continuity, momentum, and energy equations, which are based on the conservation of mass, momentum, and energy, respectively. The conservation of mass states that mass is not created or destroyed. The basic conservation relationship is the net mass flow through the faces of a small fluid element, which is equal to the time rate of mass increase inside the fluid element. The momentum equation is based on the Navier-Stokes equation that applies Newton's second law ($f = ma$), where the time rate of change of momentum of the system is equal to the sum of external forces acting on the system. The energy equation is derived and based on the first law of thermodynamics, where the rate of change of energy in a fluid element is equal to the combination of the rate of work done on a fluid element and the net flux of heat into the element (i.e., energy cannot be created, but can transform from one form into another). All these governing equations have a significant effect on CFD software, which is needed to solve the problem in a flow field based on the boundary conditions applied.

3.4.1.5 Turbulence Modeling

Turbulence modelling is one of the important elements in CFD codes, as most engineering cases or problems are associated with turbulent flow. Turbulent flow occurs at a high Reynolds (Re) number, and this dimensionless equation is used to determine the flow arrangement of fluid flow. The Re number is calculated using Equation 3.3. The types of flow can be classified into laminar ($Re < 2,300$), transient ($2,300 < Re < 4,000$), and turbulent ($Re > 4,000$). Hence, turbulence modelling is needed to solve the flow

pattern problem where several turbulence models are available, for instance, Reynolds-averaged Navier-Stokes (RANS), large eddy simulation (LES), and direct numerical simulation (DNS). Each model has its own specialty and disadvantages based on different cases.

$$\text{Re} = \frac{\rho v L}{\mu} = \frac{v L}{\nu} \quad 3.3$$

There are three types of commonly used turbulent models under RANS for flow simulation: $k - \varepsilon$, $k - \omega$, and shear stress transport (SST) $k - \omega$. Each model has its own function. The $k - \varepsilon$ model has better accuracy prediction far from the wall, whereas the $k - \omega$ model is better for the prediction near the wall. Meanwhile, the SST $k - \omega$ turbulence model can be used to combine both near and far from wall situations. In this study, the $k - \varepsilon$ turbulence model was used in the turbulent flow analysis characterised by the field of fluctuation velocity.

3.4.1.6 Turbine (Power Generation) Modeling

The value of the mechanical power can be calculated using Equation 3.5, which is the function of torque and rotational speed of the AST. The torque results were generated from the numerical simulation results as stated in Equation 3.4:

$$\tau_{screw} = \tau_p - \tau_v \quad 3.4$$

Where τ_{screw} is the torque generated, τ_p is the motor torque produced due to the pressure exerted by the flow on the blade surface, and τ_v is the brake torque due to the fluid viscosity. In this simulation, the results of the torque generated are already considered, both from motor and brake torque.

3.4.2 Meshing Sensitivity

Performing the non-dependency test is an important step in performing numerical simulation. In this project, mesh sensitivity was evaluated to identify the effect of mesh

size on the torque generated. For this analysis, five meshing sizes were evaluated (138,869; 236,012; 338,911; 453,432; and 525,440 nodes) with a constant flow rate (0.0012 m³/s), angle of inclination (30°), and rotational speed (146 rpm). All these geometries and boundary conditions used were based on the experimental setup of a previous study (Erinofiardi et al., 2017). For the experimental results, the torque generated was 0.09 Nm, which is slightly different from the numerical results, where the torque generated was 0.095 Nm.

As shown in Table 3.4, the percentage error between nodes decreases for a finer mesh. For the simulation with 100,000 to 500,000 nodes, the torque generated is mostly similar. However, the percentage error is the lowest for 500,000 nodes or more. In some cases, bigger nodes are advantageous, as the completion time of a simulation is shorter than with smaller nodes. In a real application, the error percentage should be considered as it significantly impacts the power output. The accuracy of simulation depends on the initial and boundary conditions for the simulation. The size of the time step should be small enough to determine the time-dependent features. The time step chosen must be suitable for the model condition. A very small step size will make the simulation longer, whereas a large step size will make the transient change insignificant. The convergence criteria are essential where the solution is similar to the exact solution under any pre-specified tolerance level. For this study, 525,440 nodes were chosen due to the lowest percentage error, where the value of the torque generated was close to the exact or experimental value. Hence, the subsequent simulation used 500,000 nodes.

Table 3.4 Torque generated from the simulation and corresponding percentage error

Mesh	Nodes	Torque, T (Nm)	Percentage error, %
1	138,869	0.097	7.22
2	236,012	0.100	10.00
3	338,911	0.101	10.89
4	453,432	0.096	6.25
5	525,440	0.095	5.95

3.4.3 Simulation Convergence Criteria

The convergence factor, which defines limiting behaviour and endless sequences towards some limits, is used to assess the simulation's dependability. Testing the RMS residuals values for momentum along the directions of u, v, and w is one approach to checking convergence. All of these directions, including the P-vol residual, converged below 10^{-4} . The residuals for velocity and pressure are shown in Figure 3.11, where the residuals should be as low as 10^{-3} as a good starting point. As a result, this simulation has been identified as being stable and accurate.

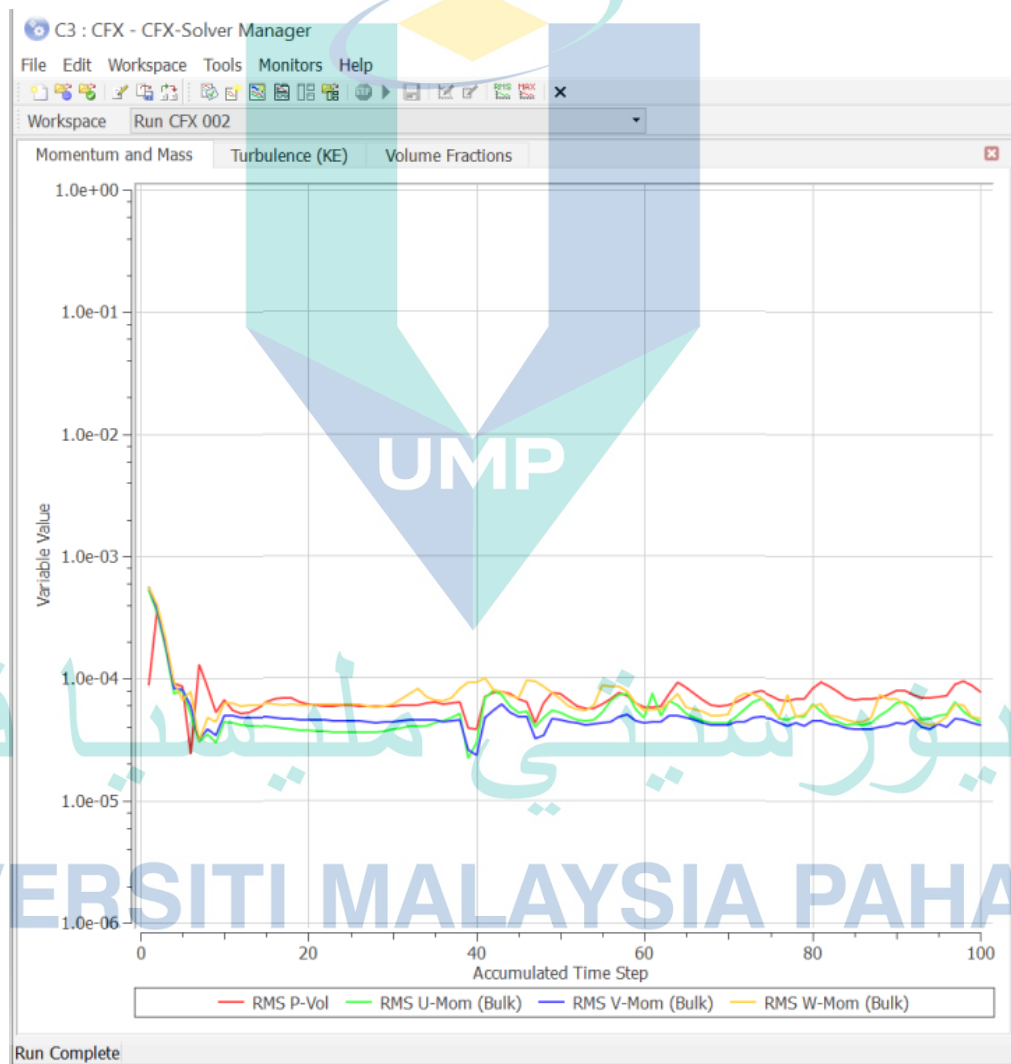


Figure 3.11 RMS Residual curve

Basically, in ANSYS, the Newton-Raphson method is used to predict the results of each iteration. For the transient simulation case, the number of iterations per time step

shows how many times the flow equations will be resolved per time step before moving on to the next time step. In this study, the time step size was 0.01 s and the total number of iterations was 100. The number of iterations depends on the application needed. The residual plot during simulation is crucial as it shows the iteration per time step. The residual curve will start at a high value at the 1st iteration and decrease with the continuity of the iterations.

The first five to ten iterations demonstrate that the solution is not too smooth, but as the number of iterations increases, the velocity and pressure curves begin to smooth out. The trend of the curve is critical for achieving the best convergence; once the curve of the graph is fixed with no or minor changes, it is considered converged. As a result, increasing the iteration step is unnecessary, as this would be counterproductive. As a result, increasing the iteration step has no effect on the obtained results.

3.5 Calculation for Power Output and Efficiency of AST

A typical example of an AST is a water inlet that enters the upper reservoirs and then travels through a bladed screw to cause it to rotate before exiting at the lower reservoir. Water that flows through the AST blade will dissipate during the rotational motion of the blade, and the difference in water level caused by the slope inclination angle will create a pressure that will generate torque. In other words, the pressure will have a trend that is directly proportional to the torque that is generated.

The hydraulic power of an AST can be determined immediately from the relationship between the rate of water flow and the difference in water pressure. In most cases, the slope inclination angle increases in direct proportion to the increase in the turbine's head difference. Equation 3.5 is used to calculate the hydraulic power of the AST.

$$P_{\text{hyd}} = \rho g Q H \quad 3.5$$

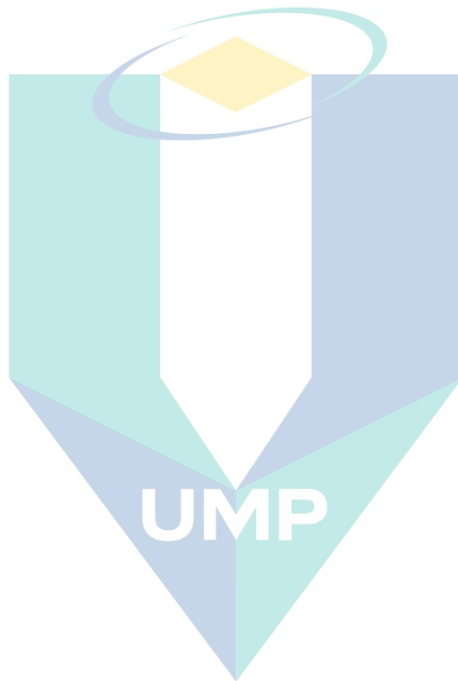
Meanwhile, torque is generated mechanically as a result of the screw rotation, resulting in force pressure on the bladed screw. The purpose of this study is to derive the

torque value from the simulation. When torque is multiplied by rotational speed, the equation for mechanical power is obtained as per Equation 3.6.

$$P_{mech} = T \cdot \omega \quad 3.6$$

The AST's efficiency can be determined using Equation 3.7 below.

$$\eta = \frac{P_{mech}}{P_{hyd}} \quad 3.7$$



اونيورسيتي مليسيا قهغ

UNIVERSITI MALAYSIA PAHANG

CHAPTER 4

RESULTS AND DISCUSSIONS

4.1 Introduction

This chapter presents the results and analysis of the power output generated and efficiency achieved by AST by using parameters such as one external parameter (slope inclination angle) and two internal parameters (number of bladed screws and diameter ratio). The design of the AST was chosen from the previous researcher's geometry (Erinofiardi et al., 2017). In this study, the simulation method is used, and before the other three parameters are simulated, the first design is validated based on the experimental results from the other researcher. Once the good agreement between these numerical and experimental parameters is achieved, the other parameters such as the slope inclination angle, α , number of bladed screws N , and the diameter ratio D_r are being investigated to identify the effect of these three design parameters on the power output and efficiency of AST.

Overall, the main research study in this thesis is regarding the design of AST. Previously, the researcher found that internal parameters have an important impact on the power output and efficiency of AST. Hence, in this research study, a combination of internal and external parameters is considered. Firstly, the literature study is reviewed and these three independent parameters are chosen. One design from the previous researcher is being studied and considered. The design is then validated between the experiment and simulation. Once the validation was done, a total of 36 simulations were run in this study using $N = 1, 2, 3$, slope inclination angle $= 20^\circ, 25^\circ, 35^\circ, 40^\circ$ with $D_r = 0.25, 0.5, 0.6$. The findings are presented and discussed in the form of power output and efficiency of AST. For further discussion, the results of power output will be separated into three sections, such as $N = 1, N = 2$ and $N = 3$. Meanwhile, the results of efficiency testing will be discussed generally.

4.2 Model Validation

The validity of the previous model from other prior studies is tested numerically using CFD. This section focused on the model validation between the simulation and the experimental results from Erinofiardi et al.,(2017). The simulation values of independent parameters were compared to data from experiments to make sure that the simulation data was correct. A fixed flow rate with various rotational speeds was used to compare the simulation values of torque to experimental data. As shown in Figure 4.1, the validation between simulation and experimental torque generated was obtained between three different values of slope inclination angles (22°, 30°, and 40°). The graph illustrates that the numerical and experimental data were in good agreement, which is within the average percentage error of 5%. However, the percentage error is quite higher at 22° compared to 30° and 40°. The percentage errors between 22°, 30°, and 40° were 20.7%, 3.8%, and 5.0%, respectively.

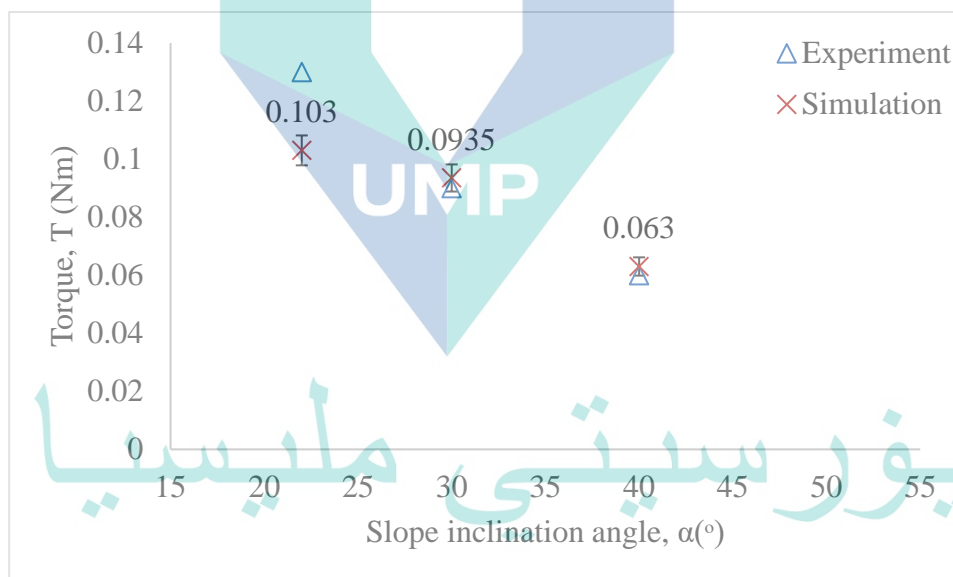


Figure 4.1 Comparison between simulation and experimental data using three different slope inclination angles

In general, as shown by the graph, the torque generated increases with decreasing slope inclination angle. In AST, the torque is generated by hydrostatic pressure, which contributes to the torque values. The power output is expected to be highest at the optimum water depth, which is at the screw's inner diameter at the widest point. In this study, the pressure exerted on the screw blades is concerning as it directly impacted the

power output of AST. In this case, the pressure exerted on the AST blades at 22°, 30°, and 40° is 217Pa, 323Pa, and 107Pa, respectively, as per Table 4.1. As a result, increasing the pressure will slow the water flow. The first blades will get the most pressure as the water flow hits the last blades.

Table 4.1 Pressure exerted on AST based on slope inclination angle

Slope inclination angle, α (°)	Pressure exerted, p(Pa)
22	217
30	323
40	107

The torque generated by varying the slope inclination was slightly different in this investigation in terms of the pressure placed on the blades. Fundamentally, the force exerted by the pressure will be precisely proportional to the torque and power created. Numerous factors affect the torque created by the applied pressure, including friction losses on the screw surface, leakage flow via the space between the blades and trough, and splashing overflow water.

In the experiment conducted by Erinofiardi et al. (2017), the hydrostatic pressure from the flowing water on the screw turbines causes the blade to rotate by using a one-bladed screw model with three different values of slope inclination angle. However, in this simulation, there are some limitations to the boundary conditions to ensure the turbine rotates due to hydrostatic force. Therefore, the simulation is set up to have a constant flow rate and rotational speed. The results in terms of torque are accumulated from the post-processing part, and the power output itself is calculated by using Equation 3.6. Besides, in this research, the bucket of the AST is assumed to have half submerged water where the boundary has been set up to have 70% air with 30% water.

4.3 Results for N=1, 2 and 3

4.3.1 At N=1

In this subchapter, screw performance was determined by simulation for different screw inclinations and diameter ratios. Figure 4.2 shows the power generated as the screw inclination angle changes for three different diameter ratios. As the slope inclination

angle increases, the power output for $0.25D_r$ decreases, but begins to increase at 40° . $0.5D_r$, on the other hand, shows that power output starts to go down at points 35° and 40° . However, the power output for $0.6D_r$ has a different trend compared to $0.25D_r$ and $0.5D_r$, which increase parallelly to the slope inclination angle. The power output trend is nearly uniform and does not differ much between the slope inclination angles.

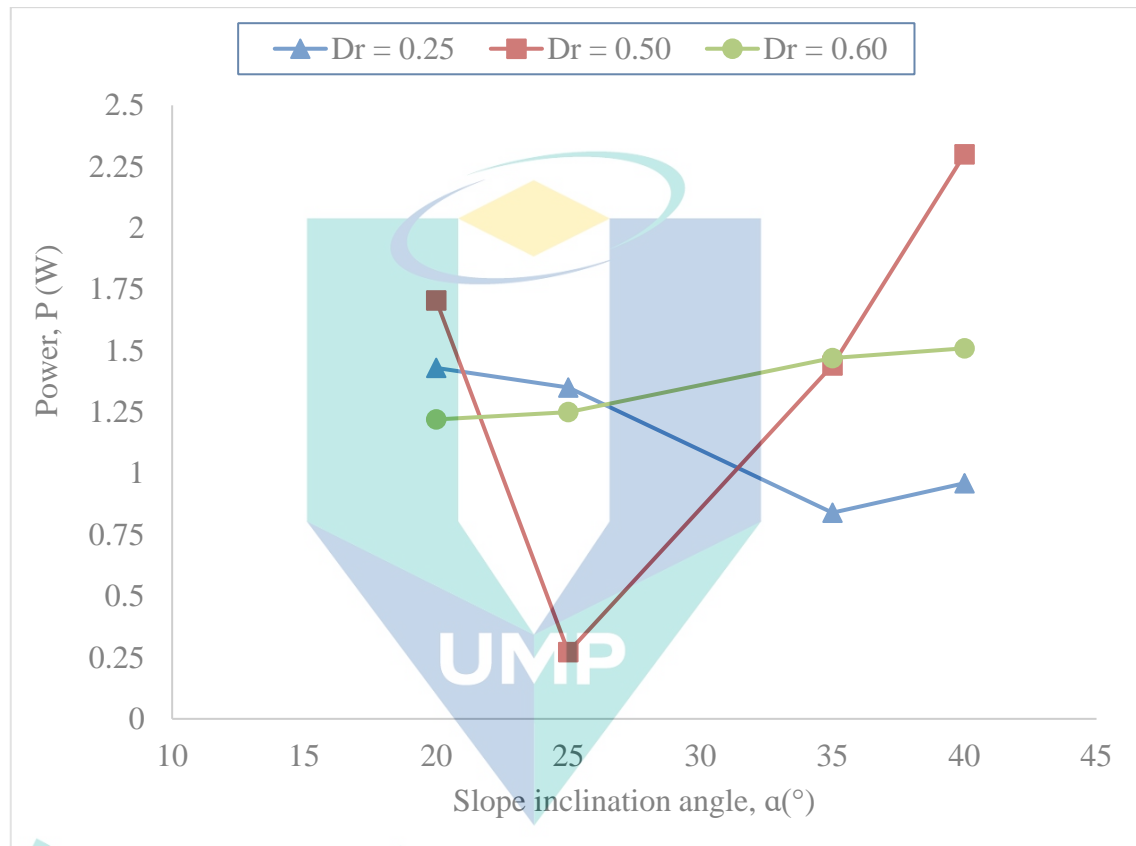


Figure 4.2 Power output of AST for different slope inclination angle and diameter ratio with constant $N=1$

The concept of AST is that water flows from the upper reservoir into the lower reservoir through the inflow, which causes the blades to rotate and generate torque. At a 1 bladed screw, the water directly hits the AST blades and creates the pressure force that acts on the blades, torque, and causes the rotation of the screw. As shown in Figure 1, at $N = 1$, the maximum power is obtained when the angle is at a high slope inclination angle and the minimum when the angle is at a low slope inclination angle. As the flow rate and the rotational speed are constant in this study, the torque generated depends totally on the water flowing that hits the blades, as each different diameter ratio and slope inclination angle have a different impact on the water when it hits the blades. Due to that, the pressure

exerted on the high reservoirs is different than the lower reservoirs. At 40° slope inclination angle and 0.5D_r, the power production of AST is maximum due to the absence of significant frictional power losses.

Mechanical power increases with the inclination angle at a specific rotation speed. The most mechanical power was identified at 40° with 0.5D_r due to the largest net water pressure applied to the blades at this inclination angle and diameter ratio. Under identical conditions (same flow rate and rotation speed), pressure and torque increase in direct proportion to the net water level differential, resulting in increased mechanical power. The highest power created by 0.25D_r occurs at a slope inclination angle of 20°, while 0.6D_r occurs at 40°. Each slope inclination angle and diameter ratio has a different effect on the amount of energy produced as impacted in terms of water pressure.

Basically, in terms of slope inclination angle, as the slope increases, the head difference of AST also increases, which may lead to some losses. At a low slope inclination angle, the water entering the turbine hits the blade with less force, at a higher slope, the water flow jumps when it passes through the inlet of AST. Lee & San Lee, (2021) found out that the findings in torque value where the maximum torque is generated at 30° and 45° slope inclination angles compared to 60°, 75°, and 90° with a varied rotational speed from 0 to 200RPM and water flow velocity of 1 to 1.5 m/s. This result shows that within the 30 to 45 range, the torque generated is at its optimum level. However, the overflow will cause a power loss in torque and power production.

4.3.2 At N=2

In this section, 12 simulations were run to study the power output generated from different angles of inclination and diameter ratios. The results of the study are as per Figure 4.3. Overall, the trend of power output is decreasing with an increase in slope inclination angle for diameter ratios of 0.25D_r and 0.6D_r, which contradicts the findings of power output for 0.6D_r. As known, the head difference increases with the slope inclination angle, and the volume of incoming water will hit the blade at a strong rate, especially at high angles. However, the number of bladed screws and the diameter ratio will to some extent affect the total volume of water that will hit the first blade, and at the

same time, affect the pressure exerted on the blade. The pressure of the blade is important in energy production as it has a direct relationship with torque.

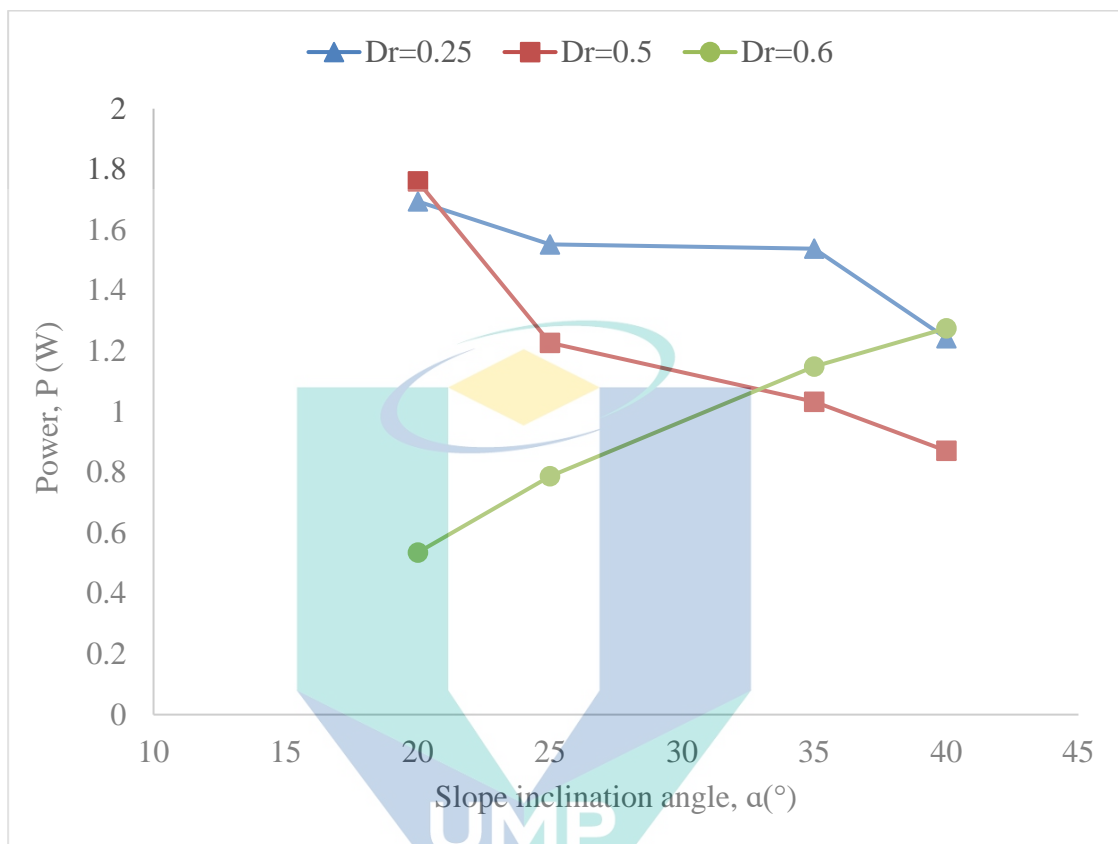


Figure 4.3 Power output of AST for different slope inclination angle and diameter ratio with constant $N=2$

At the AST's lowest power output, the reason could be due to the overflowing phenomenon that occurs at a higher inclination angle. Overflowing occurs when the flow of water through the screw exceeds the bucket's maximum volume. The overflow results in a loss of power, which prevents the screw from rotating and causes the water to splash instead of flowing through the successive blades, which results in pressure exertion. With a low inclination angle, if the water flow is not enough to make the blade rotate, an under-filled condition happens, which lowers the pressure in the water and leads to a decrease in power production.

Maulana et al.,(2019)concludes that low rotational speed is needed to ensure the higher torque generated for the high flow rate. The power production depends on the torque generated and is parallel to the pressure exerted on the blades. As the slope

inclination angle increases, the torque will decrease at constant flow rate and rotational speed due to the load that acts on the surface blade at a lower point.

4.3.3 At N=3

In this section, the simulation results of power output using three-bladed screws are discussed. The slope inclination angle and the diameter ratio value are similar to the previous section (20°, 25°, 35°, 40°, and $D_r=0.25, 0.5, \text{ and } 0.6$). Figure 4.4 shows the calculated power output generated by AST at N=3. As shown, the power decreases with an increase in slope inclination angle for $D_r=0.25$ and 0.5. However, the trend of power is different at $D_r=0.6$ as it has a decreasing trend and starts to increase at 35° and 40°. Obviously, from the graph, the maximum power is generated at a design of $D_r=0.25$ and at 20° slope inclination angles, with a minimum of $D_r=0.6$ and 25°.

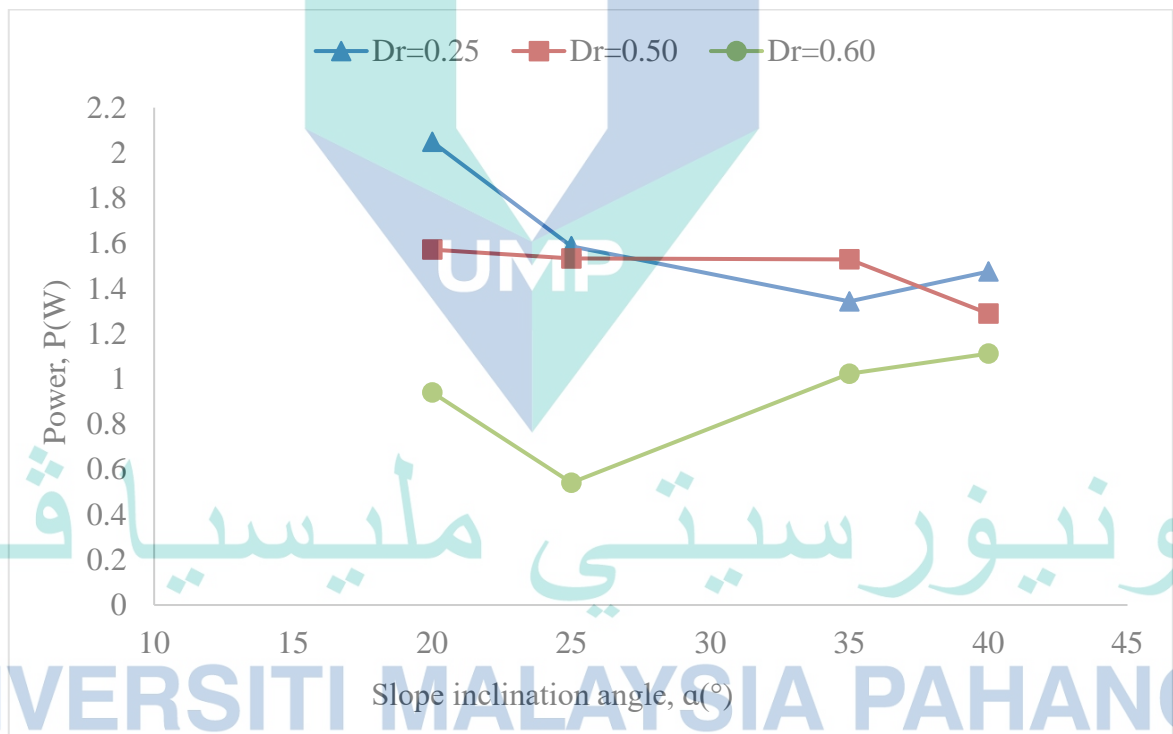


Figure 4.4 Power output of AST for different slope inclination angle and diameter ratio with constant N=3

In this study, the water flow rate and the rotational speed are constant at $0.0012\text{m}^3/\text{s}$ and 146RPM, respectively. The optimal design of AST for this configuration has been identified based on the setting. This section discussed the finding (N=3) that by increasing the number of bladed screws, the screw's number of flights increases, allowing

the screw to hold a greater volume of water (insert citation). The torque generated is proportional to the AST's power output. As the inclination of the slope increases, so does the head difference. Increases in slope inclination angle typically result in losses due to screws operating in over-filled conditions. Additionally, the pressure applied to the AST blade surface has a significant effect.

The results show the maximum power output occurred at a low slope inclination angle and a low diameter ratio. These conditions work well where a volume of water enters the turbine blade and causes the pressure exerted on the blade to great performance. Findings by Dellinger et al., (2019) found that the power output was highest (34W) at 20° to 25° with a varied water flow rate. The power output for previous findings is quite high due to the size and dimension of the AST design and the variance of the flow rate applied from 0.008 m³/s to 0.009 m³/s at each different angle.

4.4 Efficiency of the AST

The efficiency of AST is based on the parameter studies shown in Table 4.2. The results are divided into three parts, such as N=1, N=2, and N=3. The maximum efficiency of this research study is 79.42% and the minimum efficiency is 8.5%. Details of the study in terms of efficiencies are discussed further in the next paragraph.

Table 4.2 Results of efficiencies based on N, Dr and α

Number of bladed screw, N	Diameter ratio, D_r	Slope inclination angle, α (°)	Efficiency, η (%)
1	0.25	20	55.41
1	0.25	25	42.13
1	0.25	35	19.29
1	0.25	40	19.66
1	0.5	20	66.09
1	0.5	25	8.49
1	0.5	35	33.07
1	0.5	40	47.11

Table 4.2 Continued

Number of bladed screw, N	Diameter ratio, D_r	Slope inclination angle, $\alpha(^{\circ})$	Efficiency, η (%)
1	0.6	20	56.94
1	0.6	25	39.01
1	0.6	35	34.68
1	0.6	40	25.05
2	0.25	20	65.66
2	0.25	25	48.44
2	0.25	35	35.32
2	0.25	40	25.45
2	0.5	20	68.22
2	0.5	25	38.29
2	0.5	35	23.71
2	0.5	40	17.83
2	0.6	20	44.53
2	0.6	25	39.79
2	0.6	35	12.29
2	0.6	40	16.11
3	0.25	20	79.42
3	0.25	25	49.53
3	0.25	35	30.85
3	0.25	40	30.21
3	0.5	20	60.93
3	0.5	25	47.84
3	0.5	35	35.11
3	0.5	40	26.40
3	0.6	20	36.44
3	0.6	25	16.88
3	0.6	35	23.49
3	0.6	40	22.78

اونیورسیتی ملیسیا قهق
 UNIVERSITI MALAYSIA PAHANG

For $N=1$, the slope inclination angle is varied directly proportional to the efficiency of AST and the maximum efficiency occurred at 20° with a $0.5D_r$ resulted in 66%. Meanwhile, the minimum efficiency is at 25° with $0.5D_r$ generating an 8.49% efficiency. As the water flow rate and the rotational speed are set constant in this study, the water that flows into the screw AST blade will be constant too for all the slope inclination angles and at different levels of diameter ratio. The optimum efficiency occurred at a low slope inclination angle, which may be due to the fewer power losses at that point, whereas as slope inclination increases, the head difference also increases. This will impact the power inlet for the AST, as from the equation of power, the head difference and flow rate play an important role in the efficiency equation. For $N=1$, the results of efficiency have a similar trend to Erinofiardi et al., (2017) about how an increase in slope inclination angle will decrease the efficiency of AST. The contradiction between this research and that of Erinofiardi et al., (2017) is the rotational speed of the turbine, where previous researchers varied the rotational speed at each slope inclination angle.

The efficiency of $N=2$ is expected to have the same trend as $N=2$ where the efficiency decreases with an increase in slope inclination angle and a decrease in diameter ratio. The maximum efficiency (68.22%) is at 20° with $0.5D_r$ and the minimum (12.29%) is at $D_r=0.6$ at 35° . This is due to the screw's filling rate increasing with the optimum of D_r and the slope inclination angle decreasing. It is important to have an optimum value of slope inclination angle as the water inlet that flows through the blades will exert pressure, torque, and power on the AST, which then impacts the efficiency of the AST. Furthermore, higher slope inclination angles are thought to be less efficient because of more gap leakage and losses. Maulana et al., (2019) experimentally studied using a 2-bladed screw by varying the rotational speed from 59 RPM to 295 RPM and the water flow rate from $0.0044\text{m}^3/\text{s}$ to $0.025\text{m}^3/\text{s}$. The maximum efficiency occurred at an average rotational speed and an average flow rate.

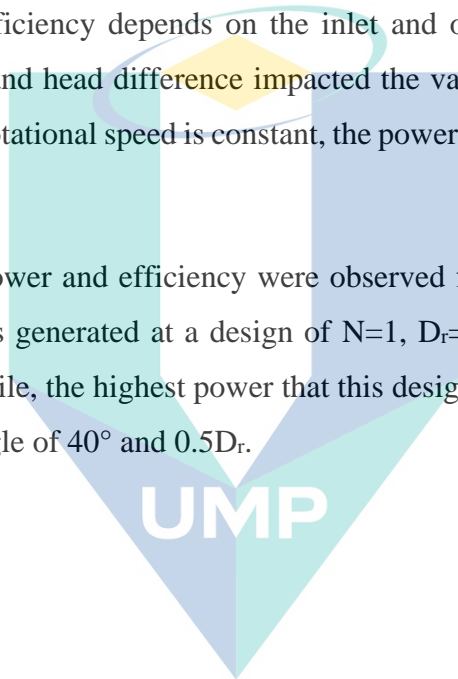
According to Table 4.2, the highest efficiency for the constant flow rate and rotational speed at $N=3$ is 79.42% at $0.25D_r$ and a low slope inclination angle of 20° for the constant flow rate and rotational speed. In the meantime, the lowest efficiency is 25° and $0.6D_r$. Basically, because the dimensions of the AST are the same, the slope

inclination angle affects the head difference of the turbine, and as hydraulic power increases as the slope inclination increases, the efficiency decreases.

4.5 Summary of the Findings

This research is about the power output and efficiency of AST by using two internal and one external parameter by simulation. The water flow rate and the AST rotational speed are set as constants, using 500k nodes of meshing, and the results of torque can be collected from the software. The power output is calculated from the torque generated, and the efficiency depends on the inlet and outlet power output. For inlet power, the flow rate and head difference impacted the value of power. Meanwhile, for output power, as the rotational speed is constant, the power output is directly proportional to the torque.

The highest power and efficiency were observed for various AST designs. The highest efficiency was generated at a design of $N=1$, $D_r=0.25^\circ$ and a slope inclination angle of 20° . Meanwhile, the highest power that this design can generate is at $N=1$, with a slope inclination angle of 40° and $0.5D_r$.



اونيورسيتي مليسيا قهغ

UNIVERSITI MALAYSIA PAHANG

CHAPTER 5

CONCLUSION AND RECOMMENDATION

5.1 Conclusion

The power output of the AST is investigated in this study using numerical simulations. When performing numerical simulation analysis, three parameters are taken into account (slope inclination angle, number of bladed screws, and the diameter ratio). The studies' conclusion is as follows:

This study showed that CFD can be used to predict the AST's power output and efficiency with high precision and at a lower cost. Optionally, based on data validation between the numerical and experimental results, the percentage error for both the 20° to 40° angles is small.

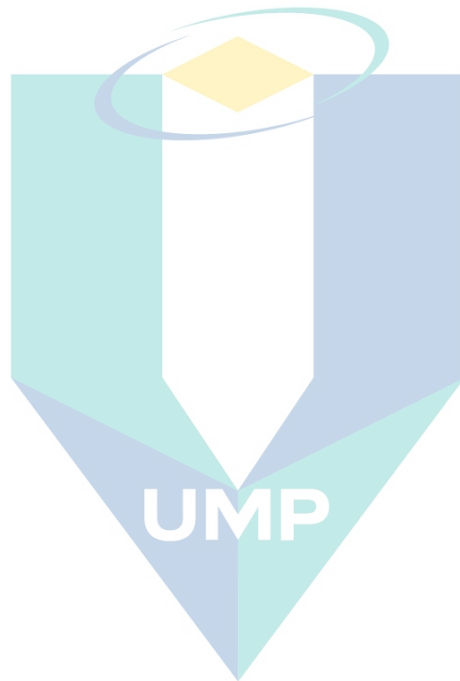
The power out of AST is calculated from the torque generated by the CFD simulation method. The maximum power output produced using this AST concept design is $\alpha=40^\circ$, $N=1$ (1-bladed), and a D_r of 0.5. Meanwhile, the efficiency is highest at $N=3$, $\alpha=20^\circ$, and $D_r=0.25$.

As a result of the results and discussion thus far, it can be concluded that a variety of factors influence the power output and efficiency of AST. CFD appears to be the best method for studying the characteristics of AST, as the flow regime of each AST system can be determined numerically. As long as the numerical and experimental results agree, it should be fine to use CFD to predict compatibility of other screw geometries without incurring excessive expense.

5.2 Recommendation

For future study, some recommendation for further research are as below; -

- i. The variation of flow rate and rotational speed of the AST can be considered to ensure that the maximum efficiency can be achieved.
- ii. The investigation of pressure exerted on each of the bladed screw and determine the best slope tilt angle of AST blade.
- iii. Simulation of AST using actual design and boundary conditions to applied in a real situation of energy conversion specially for rural area.
- iv. To investigate on the effect of other parameter such as length of the blade, number of helix screw, pitch of the screw.



اونيورسيتي ملايسيا قهغ

UNIVERSITI MALAYSIA PAHANG

REFERENCES

- Bambang Yulistiyanto, Yul Hizhar, and L. (2012). Effect of Flow Discharge and Shaft Slope of Archimedes Screw Turbine on the Micro Hydro Power Plant. *Dinamika TEKNIK SIPIL*, 12(1).
- Baños, R., Manzano-Agugliaro, F., Montoya, F. G., Gil, C., Alcayde, A., & Gómez, J. (2011). Optimization methods applied to renewable and sustainable energy: A review. In *Renewable and Sustainable Energy Reviews* (Vol. 15, Issue 4). <https://doi.org/10.1016/j.rser.2010.12.008>
- Barelli, L., Liucci, L., Ottaviano, a., & Valigi, D. (2013). Mini-hydro: A design approach in case of torrential rivers. *Energy*, 58, 695–706. <https://doi.org/10.1016/j.energy.2013.06.038>
- Bilotta, G. S., Burnside, N. G., Turley, M. D., Gray, J. C., & Orr, H. G. (2017). The effects of run-of-river hydroelectric power schemes on invertebrate community composition in temperate streams and rivers. *PLoS ONE*, 12(2). <https://doi.org/10.1371/journal.pone.0171634>
- Borhanazad, H., Mekhilef, S., Saidur, R., & Boroumandjazi, G. (2013). Potential application of renewable energy for rural electrification in Malaysia. *Renewable Energy*, 59. <https://doi.org/10.1016/j.renene.2013.03.039>
- Brada, K. (1999). *Hydraulic screw generates electricity from micro hydropower stations*. 14, 52–56.
- Chong, C., Ni, W., Ma, L., Liu, P., & Li, Z. (2015). The use of energy in Malaysia: Tracing energy flows from primary source to end use. *Energies*, 8(4). <https://doi.org/10.3390/en8042828>
- Chong, H. Y., & Lam, W. H. (2013). Ocean renewable energy in Malaysia: The potential of the Straits of Malacca. In *Renewable and Sustainable Energy Reviews* (Vol. 23). <https://doi.org/10.1016/j.rser.2013.02.021>
- Date, A., & Akbarzadeh, A. (2009). Design and cost analysis of low head simple reaction hydro turbine for remote area power supply. *Renewable Energy*, 34(2), 409–415. <https://doi.org/10.1016/j.renene.2008.05.012>
- Dellinger, G., Garambois, P. A., Dellinger, N., Dufresne, M., Terfous, A., Vazquez, J., & Ghenaim, A. (2018). Computational fluid dynamics modeling for the design of Archimedes Screw Generator. *Renewable Energy*, 118. <https://doi.org/10.1016/j.renene.2017.10.093>
- Dellinger, G., Simmons, S., Lubitz, W. D., Garambois, P. A., & Dellinger, N. (2019). Effect of slope and number of blades on Archimedes screw generator power output. *Renewable Energy*, 136. <https://doi.org/10.1016/j.renene.2019.01.060>

- Elbatran, A. H., Yaakob, O. B., Ahmed, Y. M., & Shabara, H. M. (2015). Operation, performance and economic analysis of low head micro-hydropower turbines for rural and remote areas: A review. In *Renewable and Sustainable Energy Reviews* (Vol. 43). <https://doi.org/10.1016/j.rser.2014.11.045>
- Erinofiardi, Nuramal, A., Bismantolo, P., Date, A., Akbarzadeh, A., Mainil, A. K., & Suryono, A. F. (2017). Experimental Study of Screw Turbine Performance based on Different Angle of Inclination. *Energy Procedia*, 110. <https://doi.org/10.1016/j.egypro.2017.03.094>
- Fiardi, E. (2014). Preliminary Design of Archimedean Screw Turbine Prototype for Remote Area Power Supply. *Journal of Ocean, Mechanical and Aerospace-Science and Engineering*, 5(March), 30–33.
- Furukawa, A., Watanabe, S., Matsushita, D., & Okuma, K. (2010). Development of ducted Darrieus turbine for low head hydropower utilization. *Current Applied Physics*, 10(2 SUPPL.). <https://doi.org/10.1016/j.cap.2009.11.005>
- Hendra, A. I. (2014). Manufacture of Screw Turbine and Placement of the Generator in the Screw Turbine Shaft Used for Small scale of Micro Hydro Electrical Generating. *International Conference on Mechanical Design, Manufacture and Automation Engineering*.
- Keawsuntia, Y. (2014). Design and test of pico crossflow turbine for the generation of electricity for use in the rural area. *Applied Mechanics and Materials*, 496–500. <https://doi.org/10.4028/www.scientific.net/AMM.496-500.605>
- Khan, A., Khattak, A., Ulasyar, A., Imran, K., & Munir, M. A. (2019). Investigation of Archimedean Screw Turbine for Optimal Power Output by Varying Number of Blades. *1st International Conference on Electrical, Communication and Computer Engineering, ICECCE 2019*. <https://doi.org/10.1109/ICECCE47252.2019.8940654>
- L. Barelli, L. Liucci, A. Ottaviano, D. V. (2013). Mini hydro: A design approach in case of torrential rivers. *Energy*, 58(September), 695–706.
- Lashofer, A., Hawle, W., & Pelikan, B. (2012). State of technology and design guidelines for the Archimedes screw turbine. *The International Journal on Hydropower & Dams, Hydro 2012 - Proceedings, October*.
- Lubitz, W. D. (2014). Gap Flow in Archimedes Screws. *CSME International Congress 2014, June*, 1–6.
- Lubitz, W. D., Lyons, M., & Simmons, S. (2014). Performance Model of Archimedes Screw Hydro Turbines with Variable Fill Level. *Journal of Hydraulic Engineering*, 1–11. [https://doi.org/10.1061/\(ASCE\)HY.1943-7900.0000922](https://doi.org/10.1061/(ASCE)HY.1943-7900.0000922).
- Lyons, M., & Lubitz, W. D. (2013). Archimedes screws for microhydro power generation. *ESFuelCell2013, 1999*, 1–7.

- Maulana, M. I., Syuhada, A., & Almas, F. (2018). Computational fluid dynamic predictions on effects of screw number on performance of single blade Archimedes screw turbine. *E3S Web of Conferences*, 67. <https://doi.org/10.1051/e3sconf/20186704027>
- McNabola, A., Coughlan, P., Corcoran, L., Power, C., Williams, A. P., Harris, I., Gallagher, J., & Styles, D. (2014). Energy recovery in the water industry using micro-hydropower: An opportunity to improve sustainability. *Water Policy*, 16(1). <https://doi.org/10.2166/wp.2013.164>
- Mekhilef, S. (2010). *Renewable energy resources and technologies practice in Malaysia*. 1–9. http://www.sciencedirect.com/science/article/B83X9-4NK4PRM-B/2/856cae10369cfe2c440fab98057c6f02%5Cnhttp://www.sciencedirect.com/science?_ob=ArticleURL&_udi=B83X9-4NK4PRM-B&_user=972049&_coverDate=04/16/2007&_alid=1335129621&_rdoc=11&_fmt=high&_orig=search&_
- Mohibullah, M. A. M. R. and M. I. A. H. (2004). Basic Design Aspects of Micro Hydro Power Plant and Its Potential Development in Malaysia. *National Power & Energy Conference Proceedings*, 220–223.
- Mohibullah, Radzi, M. A. M., & Hakim, M. I. A. (2004). Basic design aspects of micro hydro power plant and its potential development in Malaysia. *National Power and Energy Conference, PECon 2004 - Proceedings*. <https://doi.org/10.1109/PECON.2004.1461647>
- Muller, G., & Senior, J. (2009). Simplified theory of Archimedean screws. *Journal of Hydraulic Research*, 47(5), 666–669. <https://doi.org/10.3826/jhr.2009.3475>
- Mutasim, M. A. N., Azahari, N. S., & Adam, A. A. A. (2013). Prediction of Particle Impact on an Archimedes Screw Runner Blade for Micro Hydro Turbine. *Applied Mechanics and Materials*, 465–466, 552–556. <https://doi.org/10.4028/www.scientific.net/AMM.465-466.552>
- Nasir, B. A. (2013). Design of Micro - Hydro - Electric Power Station. *International Journal of Engineering and Advanced Technology*, 2(5), 39–47.
- Nasir, B. A. (2014). Design Considerations of Micro-hydro-electric Power Plant. *Energy Procedia*, 50, 19–29. <https://doi.org/10.1016/j.egypro.2014.06.003>
- Ong, H. C., Mahlia, T. M. I., & Masjuki, H. H. (2011). A review on energy scenario and sustainable energy in Malaysia. In *Renewable and Sustainable Energy Reviews* (Vol. 15, Issue 1). <https://doi.org/10.1016/j.rser.2010.09.043>
- Prasad, V., Gahlot, V. K., & Krishnamachar, P. (2009). CFD approach for design optimization and validation for axial flow hydraulic turbine. *Indian Journal of Engineering and Materials Sciences*, 16(August), 229–236.
- Raza, A., & Mian, M. S. (2013). *A Micro Hydro Power Plant for Distributed*

Generation using Municipal Water Waste with Archimedes Screw. 66–71.

Rohmer, J., Knittel, D., Sturtzer, G., Flieller, D., & Renaud, J. (2016). Modeling and experimental results of an Archimedes screw turbine. *Renewable Energy*, 94. <https://doi.org/10.1016/j.renene.2016.03.044>

Rorres, C. (2000). THE TURN OF THE SCREW : OPTIMAL DESIGN OF AN ARCHIMEDES SCREW. *Journal of Hydraulic Engineering*, 126(January), 72–80.

Saroinsong, T., Soenoko, R., Wahyudi, S., & Sasongko, M. N. (2015). The effect of head inflow and turbine axis angle towards the three row bladed screw turbine efficiency. *International Journal of Applied Engineering Research*, 10(7).

Saroinsong, T., Soenoko, R., Wahyudi, S., & Sasongko, M. N. (2016). Fluid Flow Phenomenon in a Three-Bladed Power-Generating Archimedes Screw Turbine. *Journal of Engineering Science and Technology Review*, 9(2). <https://doi.org/10.25103/jestr.092.12>

Shahverdi, K., Loni, R., Ghobadian, B., Gohari, S., Marofi, S., & Bellos, E. (2020). Numerical Optimization Study of Archimedes Screw Turbine (AST): A case study. *Renewable Energy*, 145. <https://doi.org/10.1016/j.renene.2019.07.124>

Shimomura, M., & Takano, M. (2013). Modeling and Performance Analysis of Archimedes Screw Hydro Turbine Using Moving Particle Semi-Implicit Method. *Journal of Computational Science and Technology*, 7(2), 338–353. <https://doi.org/10.1299/jcst.7.338>

Siswantara, A. I., Warjito, Budiarso, Harmadi, R., Gumelar, M. H., & Adanta, D. (2019). Investigation of the α angle's effect on the performance of an Archimedes turbine. *Energy Procedia*, 156. <https://doi.org/10.1016/j.egypro.2018.11.084>

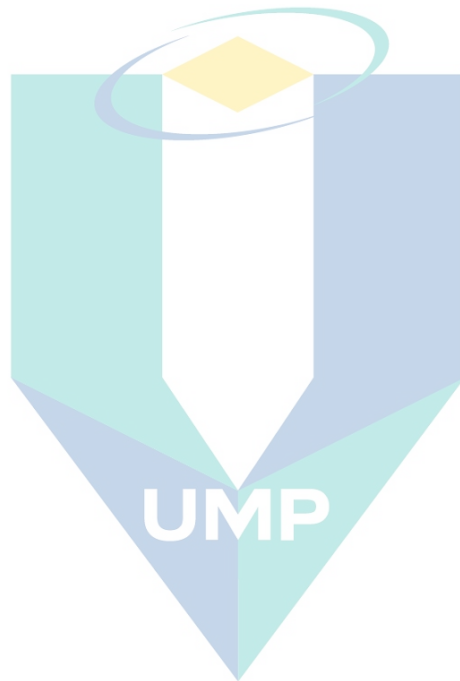
Stergiopoulou, A, Stergiopoulos, V., Kalkani, E., & Education, T. (2013). *CONTRIBUTIONS TO THE STUDY OF HYDRODYNAMIC BEHAVIOUR OF INNOVATIVE ARCHIMEDEAN SCREW TURBINES RECOVERING THE HYDROPOTENTIAL OF WATERCOURSES AND OF COASTAL CURRENTS.* September, 5–7.

Stergiopoulou, Alkistis, & Kalkani, E. (2013). Investigating the Hydrodynamic Behavior of Innovative Archimedean Hydropower Turbines. *International Journal of Research and Reviews in Applied Sciences*, 17(November), 87–96.

Tu, J., Yeoh, G. H., & Liu, C. (2018). Computational fluid dynamics: A practical approach. In *Computational Fluid Dynamics: A Practical Approach*.

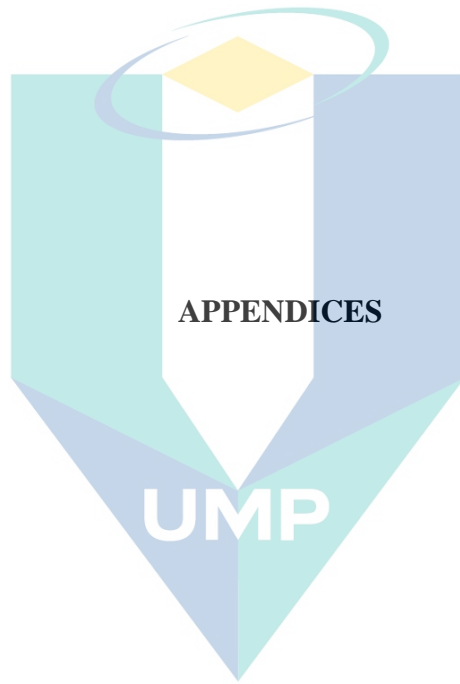
Wang, J. F., Piechna, J., & Müller, N. (2012). A novel design of composite water turbine using CFD. *Journal of Hydrodynamics*, 24(1). [https://doi.org/10.1016/S1001-6058\(11\)60213-8](https://doi.org/10.1016/S1001-6058(11)60213-8)

Waters, S., & Aggidis, G. A. (2015). Over 2000 years in review: Revival of the



اونيورسيتي ملايسيا قهغ

UNIVERSITI MALAYSIA PAHANG



اونيورسيتي ملايسيا قهغ

UNIVERSITI MALAYSIA PAHANG

Appendix A: List of Paper Published

The list of papers published are as follows:

1. A. Nurul Suraya, N. M. M. Ammar and J. Ummu Kulthum, The Effect of Substantive Parameters On The Efficiency Of Archimedes Screw Microhydro Power: A Review. IOP Conf. Series: Materials Science and Engineering 100 (2015). pp. 1-9. ISSN 1757-8981.
2. C. Zafirah, Rosly and U. K., Jamaludin and Nurul Suraya, Azahari (2016) Parametric Study on Efficiency of Archimedes Screw Turbine. ARPN Journal of Engineering and Applied Sciences, 11 (18). pp. 10904-10908. ISSN 1819-6608.
3. Nurul Suraya, Azahari and U. K., Jamaludin and N. M. M., Ammar (2016) Investigation on the Effect of Drive Train System for Archimedes Screw Turbine. In: The 4th International Conference on Engineering and ICT (ICEI 2016), 4-6 April 2016, Melaka, Malaysia. pp. 1-5.

UMP

اونيورسيتي ملايسيا قهغ

UNIVERSITI MALAYSIA PAHANG